The role of emission reductions and the meteorological situation for air quality improvements during the COVID-19 lockdown period in Central Europe

Volker Matthias[1], Markus Quante[1], Jan A. Arndt[1], Ronny Badeke[1], Lea Fink[1], Ronny Petrik[1], Josefine Feldner[1], Daniel Schwarzkopf[1], Eliza-Maria Link[1], Martin O.P. Ramacher[1], Ralf Wedemann[1]

[1]Helmholtz-Zentrum Hereon, Max-Planck-Straße 1, 21502 Geesthacht, Germany

Correspondence to: Volker Matthias (volker.matthias@hereon.de)

Abstract. The lockdown measures taken to prevent a rapid spreading of the Corona virus in Europe in spring 2020 led to large emission reductions, particularly in road traffic and aviation. Atmospheric concentrations of NO_2 and $PM_{2.5}$ were mostly reduced when compared to observations taken for the same time period in previous years, however, concentration reductions may not only be caused by emission reductions but also by specific weather situations.

In order to identify the role of emission reductions and the meteorological situation for air quality improvements in Central Europe, the meteorology chemistry transport model system COSMO-CLM/CMAQ was applied to Europe for the period 1 January to 30 June 2020. Emission data for 2020 was extrapolated from most recent reported emission data and lockdown adjustment factors were computed from reported activity data changes, e.g. google mobility reports. Meteorological factors were investigated through additional simulations with meteorological data from previous years.

The results showed that lockdown effects varied significantly among countries and were most prominent for NO_2 concentrations in urban areas with two-weeks-average reductions up to 55% in the second half of March. Ozone concentrations were less strongly influenced (up to +/- 15%) and showed both increasing and decreasing concentrations due to lockdown measures. This depended strongly on the meteorological situation and on the NOx/VOC emission ratio. $PM_{2.5}$ revealed 2-12% reductions of two-weeks-average concentrations in March and April, which is much less than a different weather situation could cause. Unusually low $PM_{2.5}$ concentrations as observed in Northern Central Europe were only marginally caused by lockdown effects.

The lockdown can be seen as a big experiment about air quality improvements that can be achieved through drastic traffic emission reductions. From this investigation, it can be concluded that NO_2 concentrations can be largely reduced, but effects on annual average values are small when the measures last only a few weeks. Secondary pollutants like ozone and $PM_{2.5}$ depend more strongly on weather conditions and show a limited response to emission changes in single sectors.

1 Introduction

The global spread of the Corona virus since the start of 2020 resulted in unprecedented emission reductions caused by lockdown measures in many parts of the world. In Europe, significant reductions in road and air traffic as well as in industrial activities began between end of February and mid of March 2020. Emissions were heavily reduced

in short time, but then steadily increased again as lockdown measures were lifted step by step, until they reached approximately previous year levels in summer (Forster et al., 2020). However, this temporal emission behaviour varied from country to country and among the different emission sectors. Emission reductions between the second half of March and end of June 2020 were probably the largest in Europe since decades, in particular in traffic. From an air quality perspective, this can be regarded as a huge real world experiment about the effects of severe emission reductions on air pollutant concentrations and possible side effects of emission reduction measures, e.g. on secondary pollution formation.

Observational data at ground level and from satellite showed large, but regionally different reductions in NO_2 concentrations (e.g. Bauwens et al. (2020);Menut et al. (2020);Velders et al. (2021);Lonati and Riva (2021). For particulate matter (PM), concentration reductions were less clear and not necessarily in line with the expectations that would follow the estimated emission reductions. Obviously, weather conditions also have a significant impact on pollutant concentration levels, but despite the high number of publications that analyse COVID-19 lockdown effects on air pollution, meteorological influences are mostly not taken into account properly (Gkatzelis et al., 2021). Wind direction determines strongly the advection of gases and aerosols from distant regions into the area of interest, higher wind speeds can activate additional emission sources like re-suspension of deposited particles, solar radiation affects photochemical reactions, and precipitation amounts control deposition.

As has been pointed out in recent publications about the effect of COVID lockdown emission reductions on air pollutant concentrations (e.g. Menut et al. (2020);Velders et al. (2021)), the relationship between emissions and concentrations is not necessarily straightforward and easy to explain. A simple comparison between before and after lockdown concentrations neglects seasonal and weather effects. A similar argument holds for comparisons with the same week of the previous year. While seasonal effects are considered in this case, the weather situation might still be very different. In addition, technology or economically driven emission changes from one year to another are not taken into account. Chemistry transport models and sophisticated emission models can help in disentangling the relationships between emissions, meteorology, and concentration levels. In addition, they can quantify the contribution of different source sectors and investigate effects of reduced concentrations of specific pollutants on the formation of other secondary species. For example, it has been discussed by Kroll et al. (2020) and Huang et al. (2020) that lower NO emissions might lead to higher ozone concentrations and a higher potential for the oxidation of organics, which might result in increased secondary organic aerosol (SOA) formation. In fact, Amouei Torkmahalleh et al. (2021) analysed observed NO_2 and O_3 concentrations in numerous cities around the world and report increased ozone in urban environments. However, depending on the NOx/VOC emission ratios and the meteorological situation, the effects might differ from place to place (see e.g. Mertens et al. (2021)).

To quantify the effects of the lockdown measure on ambient concentrations, these need to be separated from other sources of influence which predominantly are assumed to be the meteorological conditions. For Europe, Menut et al. (2020) assessed the influence of lockdown measures on air quality without the biases of meteorological conditions in an ad-hoc modelling study for March 2020. They compared a reference model run with 2017 emission data for Europe to a lockdown run with estimated emission reductions. Both runs were based on the same meteorological fields. Considerable decreases in NO_2 concentrations due to the lockdown measures alone have been found. The effect on fine particle concentrations has been comparably less pronounced (−5 to −15%). Sharma et al. (2020) performed a similar study for India, they reported a remarkable increase in O_3. With focus on the Netherlands, Velders et al. (2021) used a machine learning (ML) algorithm to remove the effects due to

meteorological variability on pollutant concentrations and applied chemical transport modelling. They concluded that the unusual 2020 meteorology in the Netherlands led to decreased PM_{10} and $PM_{2.5}$ concentrations but the NO_2, and O_3 concentrations were not affected. In a study addressing the air quality during the lockdown period in Milan Collivignarelli et al. (2020) eliminated the influence of weather phenomena on the air quality by identifying a meteorological reference period. Using machine-learning (ML) models fed by meteorological data Petetin et al. (2020) estimated the NO_2 mixing ratios for Spain that would have been observed in absence of the lockdown. It was found that the lockdown measures were responsible for a 50% reduction in NO_2 levels. Goldberg et al. (2020) showed that accounting for meteorological influences is important when satellite data is used to estimate the drops in columnar NO_2 in the United States. And, van Heerwaarden et al. (2021) used ground based and satellite observations in combination with radiative transfer modelling to disentangle meteorological effects and those of aerosol emissions. They concluded that lockdown measures were far less important for the irradiance record than the exceptionally dry and particularly cloud-free weather.

In this paper we present results derived with the COSMO-CLM/CMAQ model system together with a highly modular emission model to quantify the contribution of the estimated emission reductions on the concentrations of NO_2, O_3 and $PM_{2.5}$ in Central Europe and to separate the contribution of emission changes from those caused by distinct weather patterns. CMAQ was fed with updated emission data for the year 2020, including time profiles for sectors and countries that approximate the lockdown emission reductions. Chemistry transport model simulations were performed for January – June 2020. The effects of distinct weather patterns on the effects of emission reductions on pollutant concentrations were investigated through additional simulations with meteorological conditions for the same time period in recent previous years with very different weather conditions. The results allow for an interpretation of the observed concentration reductions when compared to previous years. It also gives a range of possible concentration changes resulting from the same emission reductions.

2 Model simulations

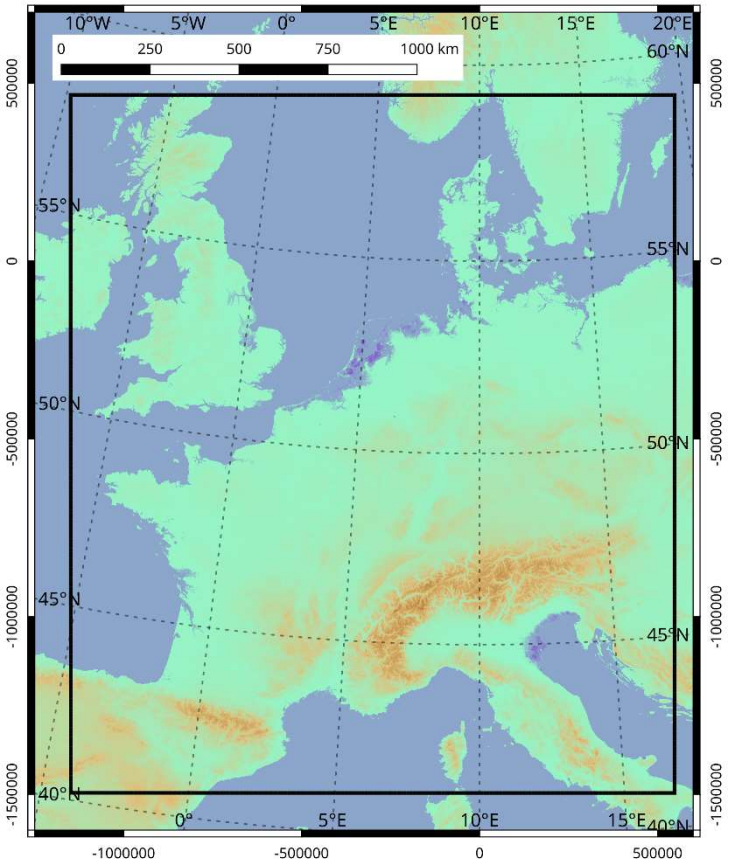

Figure 1: Inner domain of the CMAQ model (black line) along with the coordinates of the CMAQ projection (values outside the zebra frame)

This study focuses on the effects of emission reductions during the lockdown in Central Europe in spring and early summer 2020. While emission changes were considered for entire Europe, the main area under investigation w.r.t. effects on concentrations covers the most populated regions in Central Europe (Fig .1), only. This restriction was applied for the sake of a higher resolution and for allowing a reasonable interpretation of meteorological impacts. The Community Multi-scale Air Quality Model (CMAQ) (Byun and Schere, 2006;Byun and Ching, 1999) version 5.2 was used with the carbon bond 5 (CB05) photochemical mechanism (CB05tucl) (Kelly et al., 2010)and the AE6 aerosol mechanism. The model was run for 2020 with a spin-up time of 2 weeks in 2019 to avoid the influence of initial conditions on the modelled atmospheric concentrations. CMAQ was set up on a 36 x 36 km^2 grid for entire Europe and for a one-way nested 9 x 9 km^2 grid for Central Europe, see Fig. 1. The vertical model extent comprises 30 layers from the model surface up to the 100 hPa pressure level. Twenty of these layers are below approx. 2000 m, and the lowest layer has a height of 36 m.

Chemical boundary conditions for the outer model domain were taken from the IFS-CAMS analysis (Inness et al., 2019b) available from the MARS archive at ECMWF and the Copernicus Atmosphere Monitoring Service Atmosphere Data Store (Inness et al., 2019a). Particle and gas concentration fields of the Global Analysis and Forecast are provided on a T511 spectral grid with 137 vertical levels. Emission changes caused by lockdown measures are not considered in this data set. The IFS-CAMS data were temporally and spatially remapped onto the boundary of the CMAQ domain. Finally, a unit conversion and a transformation of the chemical species from IFS-CAMS to CMAQ were applied.

Meteorological data for the CMAQ model were provided by a simulation of the COSMO model (Baldauf et al., 2011;Doms et al., 2011;Doms and Schättler, 2002) applying the version COSMO5-CLM16 (climate mode (Rockel et al., 2008)). To simulate the radiative transfer as realistic as possible, an extension of the COSMO model for the MACv2 transient aerosol climatology was used. The soil was initialized taking the data from a 40 year simulation with the COSMO model. Then, the atmospheric simulations were performed for the period 1 September 2019 to 30 June 2020 using the MERRA2 Global reanalysis (Gelaro et al., 2017) as initial and lateral boundary conditions. The same was done for the periods 1 September 2015 to 30 June 2016 and 1 Sep 2017 to 30 June 2018. To ensure that the atmospheric fields in the transient model integration are close to the observations over the whole period of 10 months, a nudging technique was used as described in Petrik et al. (2021). The reader is referred to this publication to find more information about the setup of the atmospheric model (setup 'CCLM-oF-SN').

CMAQ simulations were performed with emissions as they could be expected for 2020 without any lockdown measures and with another emission data set that was modified according to reported changes in traffic and industrial activities. The latter is regarded as the emission data set that best reproduces real world emissions during the first COVID-19 lockdown phase in 2020. In the following we will refer to this simulation as the COV case, while the simulations with expected emissions without lockdown is referred to as the noCOV case. The difference between the simulated pollutant concentrations for the two cases represents the COVID-19 lockdown effects on air quality. A detailed description of the emission data construction is given in the next section. Additional model simulations with meteorological conditions for the years 2016 and 2018 have been performed with CMAQ using the same 2020 emission data sets.

3 Emission data

3.1 Basic emissions 2020, noCOV case

Emissions are based on the CAMS-REGAP-EU version 3.1 available at the ECCAD website (https://permalink.aeris-data.fr/CAMS-REG-AP). The dataset comprises annual totals for anthropogenic emissions in 13 GNFR sectors (Granier et al., 2019). The most recent data set was for 2016. For this study, the emission data was extrapolated to the year 2020 based on the temporal emission development in previous years.

For the application in the CMAQ model the data was re-gridded and vertically and temporally redistributed. Additionally, in order to investigate the effects of lockdown measures on the emissions, sector and country specific temporal profiles of lockdown effects were applied. The data preparation was done with a modular toolbox for emission calculation, the Highly Modular Emission MOdel (HiMEMO), currently developed at Helmholtz-Zentrum Hereon. The framework is built in the R programming language, using the libraries netcdf, proj4, sp, raster and their dependencies.

HiMEMO was run with gridded emission data from the CAMS inventory for 2016 in a spatial resolution of 0.05° x 0.1°. The inventory contains gridded annual emissions for chemical species groups, i.e. NO_x, NMVOC, CO, NH_3, CH_4, SO_2, $PM_{2.5}$ and PM_{10}. Several of these chemical groups need to be split into chemical components, or sub-groups of species according to the CB05 chemical mechanism used by CMAQ. The NO_x split was done by applying a NO/NO_2 ratio of 90/10 for traffic, a ratio of 92/8 for shipping and 95/5 for all other sectors. Land based NMVOC emissions were split for individual sectors according to a split provided by TNO (J. Kuenen, pers.

communication). PM was split as described by Bieser et al. (2010) for the SMOKE for Europe emission model. All other species in the CAMS-REGAP-EU inventory were directly transferred to CMAQ.

Vertical emission distributions per sector follow Bieser et al. (2011). The vertical distribution for the shipping sector was treated differently for land and ocean-going ships, the latter being emitted in altitudes up to 100 m. The temporal profiles follow those provided by TNO (Denier van der Gon et al. (2011), also described in Matthias et al. (2018)).

Biogenic emissions of VOCs (BVOCs) and NO were calculated with the Model of Emissions of Gases and Aerosols from Nature (MEGAN) (Guenther et al., 2012). Version 3 of MEGAN (Guenther et al., 2020) was used in this study, it was driven by preprocessed meteorological data for CMAQ as described above. Vegetation data tables were downloaded from the MEGAN website and not further modified for this study. Leaf area index (LAI) data was taken from GEOV1 products (SPOT/PROBA V LAI1) as an alternative input for MEGAN3 (Baret et al., 2013).

The annual emission data for 2016 were extrapolated to 2020 for each national emission sector according to the Gridded Nomenclature For Reporting (GNFR) in order to produce expected emissions for 2020 without lockdown effects. The starting point were the time series data of yearly totals for the pollutants BC, CO, NH_3, NMVOC, NO_x, PM_{10}, $PM_{2.5}$ and SO_2, which are provided by the EMEP centre on emission inventories and projections (EMEP/CEIP 2020 Present state of emission data; https://www.ceip.at/webdab-emission-database/reported-emissiondata). Using the time series data, a mean annual change rate for emissions (CE, in %) was derived for each pollutant, sector and country, separately. The projection of the 2016 emissions to the year 2020 was realized through a projection factor PF=1+ CE/100*(2020-2016). Using a mean change rate based on the development of emissions within the 3 years 2017-2019 (method 1), PF could be very large (more than 2) for some countries and sectors. This can result from large changes and fluctuating time series of the yearly emissions. In order to avoid very large and presumably erroneous emission changes between 2016 and 2020, a maximum allowed annual change rate was introduced. If the CE was larger than 10%, a modified CE was computed by considering the entire time series of annual emissions, but not more than ten years (method 2). If there still was a CE of more than 10%, we limited it to a maximum change of ±10%. Regarding the shipping sector, no changes were assumed between the years 2016 and 2020.

3.2 Lockdown effects, COV case

For the lockdown scenario, we adjusted national emissions from the following GNFR sectors: A_PublicPower, B_Industry, F_RoadTransport, G_Shipping and H_Aviation. Lockdown emission reduction functions, here called Lockdown Adjustment Factors (LAF) were calculated based on published data sources that resemble the effects of lockdown measures on a daily basis. LAFs were derived for 42 European countries and two sea basins, the North Sea and the Baltic Sea.

The datasets used for the construction of the LAFs are described in the following. If the input data was not available for an individual country, data from a neighbouring country was used to estimate the reduction. A table showing the data availability per sector and country is given in the appendix (Table A1). The LAFs are applied to all species, heights and time steps of the anthropogenic emission dataset for 2020.

A_PublicPower and B_Industry

Eurostat data (https://ec.europa.eu/eurostat/databrowser/view/sts_inpr_m/default/bar?lang=en) was used to account for changes in the sectors A_PublicPower and B_Industry. The energy data provided there comprise monthly information on the volume index of production for electricity, gas, steam and air conditioning supply. They are available for 35 countries in Europe. The industry data comprise monthly information on the volume index of production for mining and quarrying; manufacturing; electricity, gas, steam and air conditioning supply and construction and are available for 20 countries in Europe. The indices are based on an index value of 2015. However, since we want to use them to evaluate the lockdown period, we normalized the changes based on the January 2020 value. The data are given in a monthly resolution, however, for many countries in Europe the lockdown started in mid of March. Therefore, a piecewise cubic spline interpolation procedure was applied to derive daily lockdown adjustment factors while still maintaining the monthly values. Examples are given for both sectors in Germany in Fig. 2.

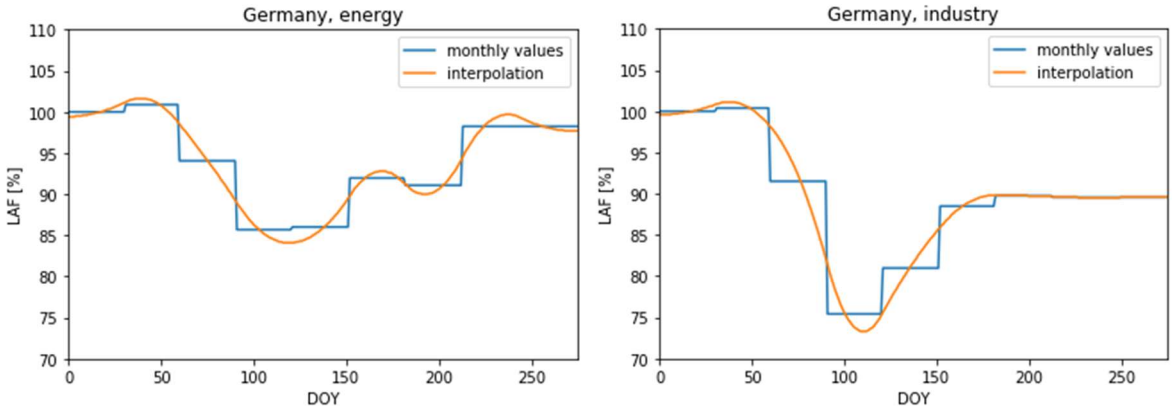

Fig. 2: Examples for monthly values and interpolated functions for Lockdown Adjustment Factors (in %) for the sectors A_PublicPower and B_Industry in Germany.

F_RoadTransport

Google Mobility Reports (https://www.google.com/covid19/mobility/) deliver daily percentage change of visits in different areas (e.g. residential, transit, recreation, work places). The reference value is the median of the corresponding weekday between 3rd of January and 6th of February 2020. We use Google Mobility Reports for transit on a national level to account for the changes in road traffic emissions. Through this method, reduced traffic on national holidays, e.g. around Easter and 1 May are considered as well, however, vehicle types cannot be distinguished.

G_Shipping

To derive scaling factors that account for ship traffic and emission reductions in this sector, bottom-up ship emission inventories were created with the MOSES ship emission model (Schwarzkopf et al., 2021) using Automatic Identification System (AIS) data for 2019 and 2020 covering the German Bight and the Western Baltic Sea. The data was recorded in Bremerhaven and Kiel by the German Federal Maritime and Hydrographic Agency (BSH). A 7-days rolling mean filter was applied to the calculated CO_2 emission ratios (Fig. 3). On average, the data revealed a slight reduction of ship traffic in the North Sea area by approx. 10%. For the Baltic Sea traffic

reductions were clearly visible with a downward trend from March until mid of June that could be mainly attributed to Roll-on/Roll-off (RoRo) ships and passenger ships. For the first 75 days of the year until 15 March 2020 no reductions were applied, afterwards daily LAF were used similar to the approach for road traffic. LAFs for the North Sea were also applied for the Mediterranean Sea, those for the Baltic Sea were also applied to inland shipping. The reasoning behind this is that shipping in the Mediterranean is mostly international cargo transport, similar to the North Sea, and inland navigation is connected to short range transport, similar to the Baltic Sea. As can be seen in Fig.3 relative increases in shipping emissions might also occur during limited time.

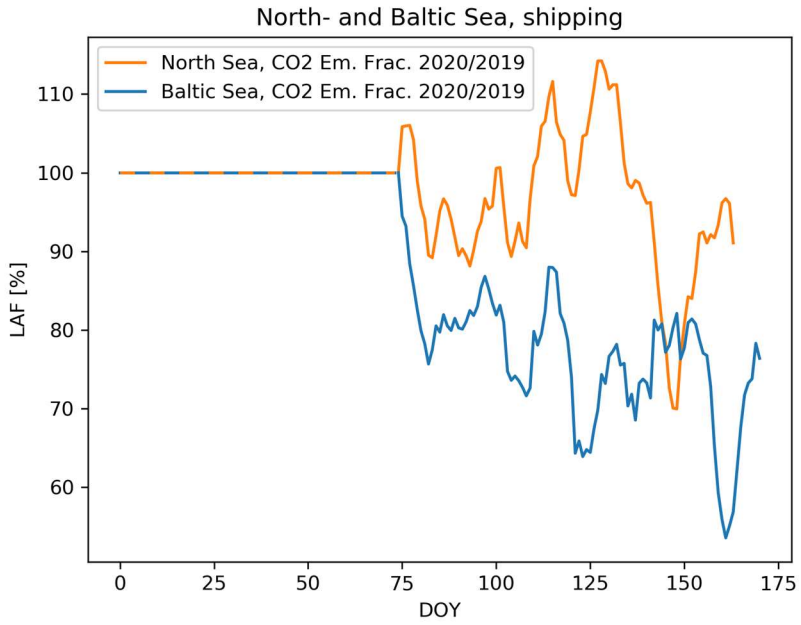

Fig 3: Lockdown adjustment factors created from the seven days rolling mean ratios of CO2 emissions from shipping in 2020 relative to 2019. Until day 75 (15 March) no changes and a LAF of 1 was assumed.

H_Aviation

Airport traffic total arrivals and departures data from Eurocontrol (https://ansperformance.eu/data) were used to account for emission changes in the aviation sector. We applied a reduction based on a weekday mean from 3 January 2020 until 6 February 2020, similar to Google mobility data. Daily values for 42 European countries are available. The relative reductions in this sector were most pronounced, reaching -90% in March and April and a slower recovery than the other sectors.

Sector Comparison

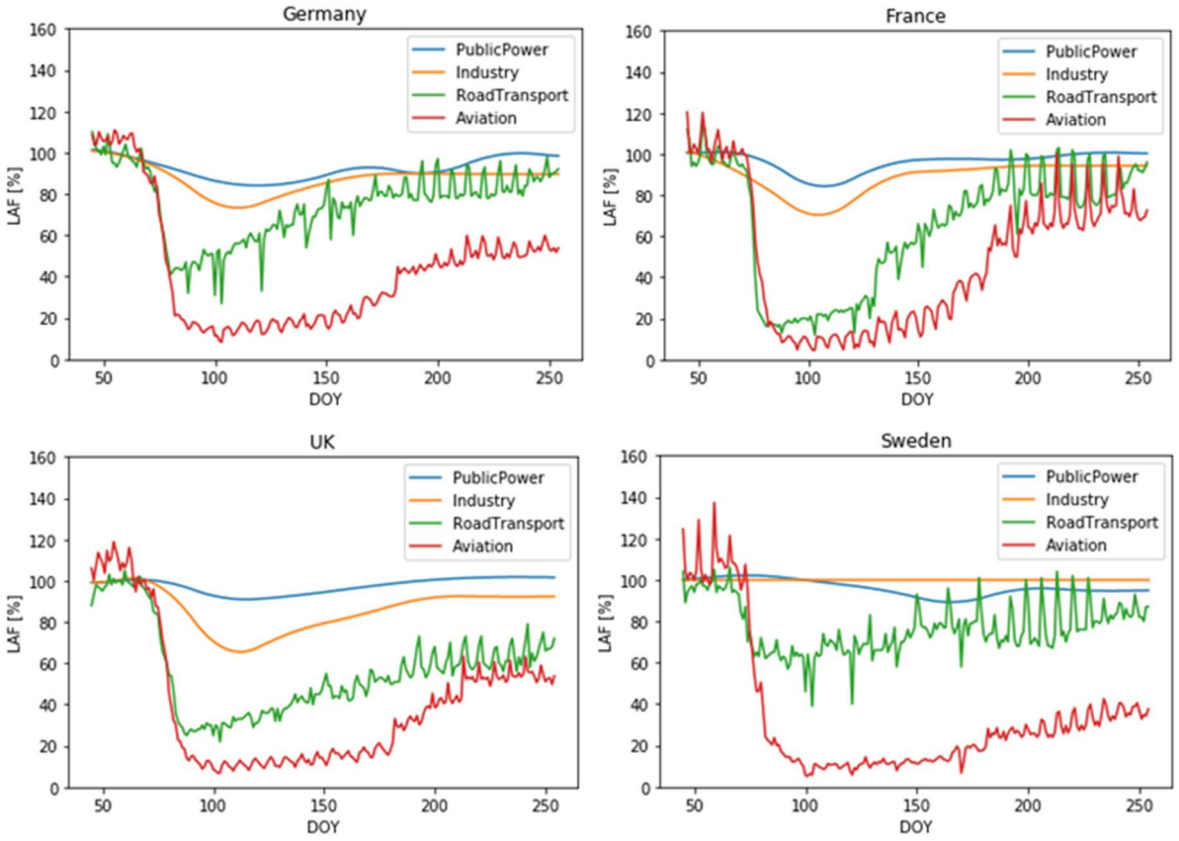

Fig. 4: LAFs for Germany (a), France (b), United Kingdom (c) and Sweden (d) for the sectors: A_PublicPower, B_Industry, F_RoadTransport, and H_Aviation

LAFs for Germany, France, UK and Sweden are exemplarily shown in Figure 4. Huge emission reductions in road traffic and air traffic between 10 and 20 March (day of the year (DOY) 70-80) can clearly be seen. Public power and industry, on the other hand, show much smaller reductions (10-30%) and almost reach previous year levels until the end of June. At the same time in France and Germany, road traffic was back to 90% of the previous year, however in the UK and in Sweden 20-40% reductions were still visible in the activity data. Comparisons of country-specific LAFs for the sectors F_RoadTransport, and H_Aviation are given in the supplement (Fig. A1 and A2).

Figure 5 presents total daily NO_x emissions in the entire Central European domain (see Fig. 1) for the time period from 1 January to 30 June 2020 for the COV and the noCOV case separated by GNFR sectors. Road transport is the most important emission sector with approx. 20 to 30%, followed by ocean shipping, other stationary combustion, industry and public power, which all have similar contributions of approx. 10%. Combustion shows a clear decline towards the summer months due to the fact that domestic heating is mainly necessary in winter. Reductions caused by the lockdown stem mostly from the road transport sector, with a strong drop in emissions starting around DOY 75 (15 March). The aviation sector, which experienced the strongest relative drop in emissions during the lockdown, does not play a major role for the overall emission of NO_x. However, it might be important near airports and in the upper troposphere. Overall, NO_x emissions in Central Europe dropped by around 25000 mol/s (approx. 4 kt/h, when given as NO_2) during the strictest lockdown period in late March and early April. This corresponds to a relative drop of around -30% (Fig. 5).

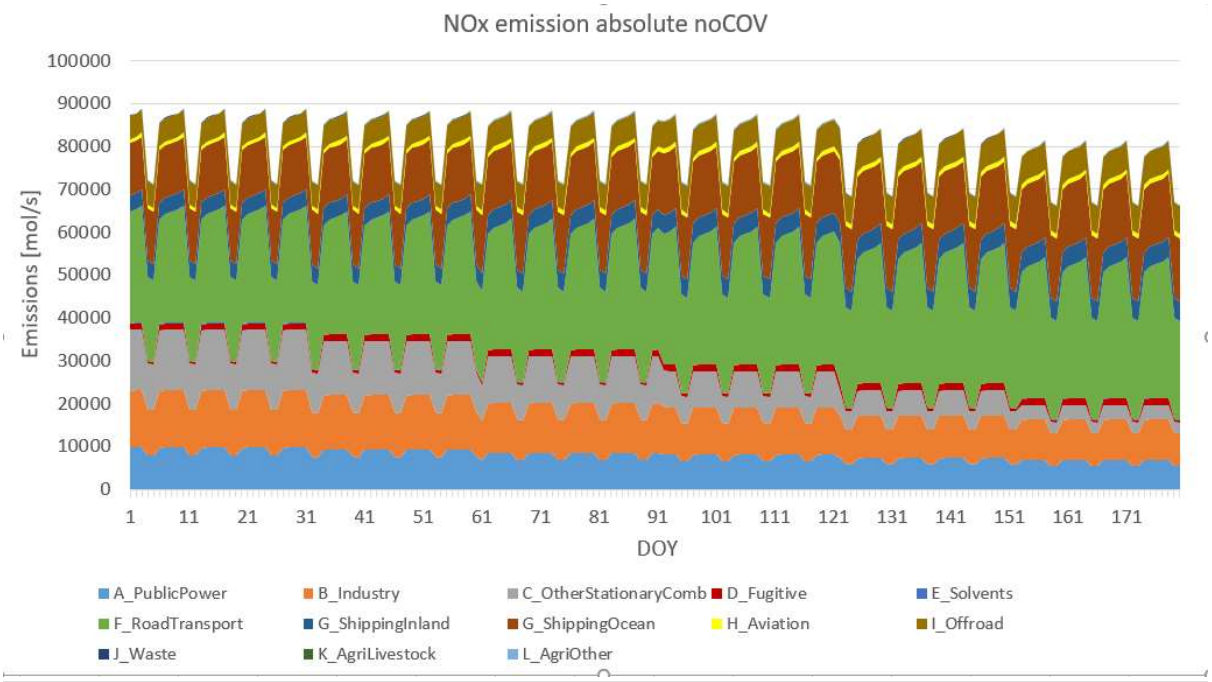

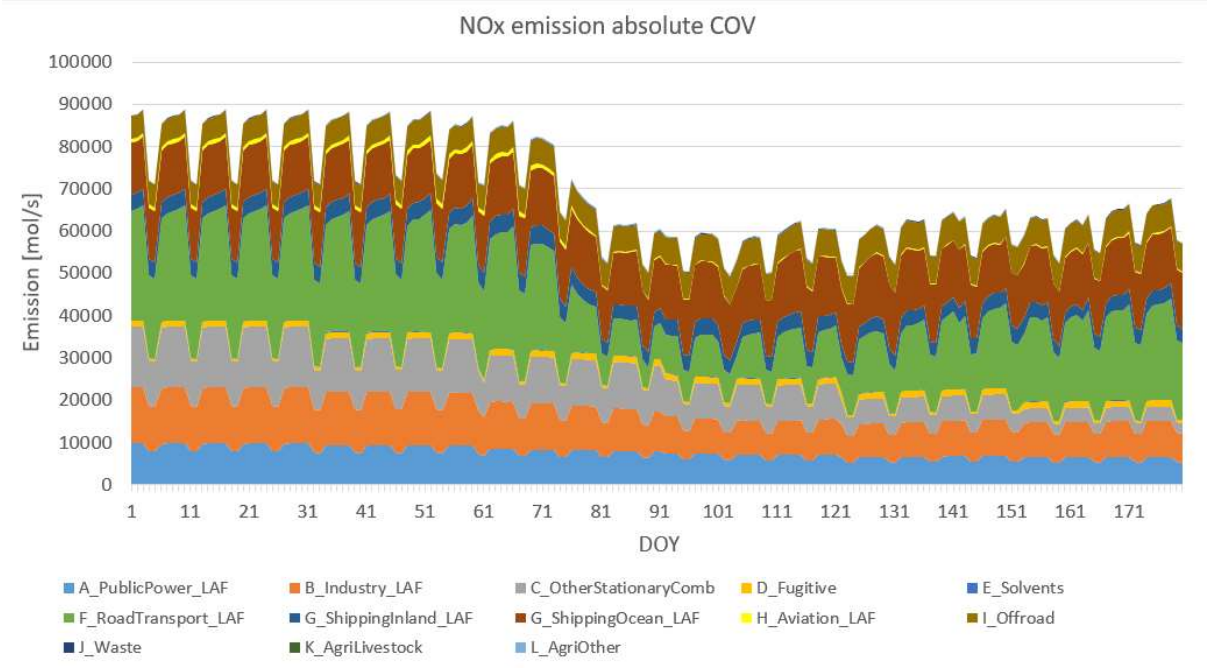

Fig.5: Daily average values for sector separated NOx emissions summarized over the entire Central European model domain for the noCOV and the COV case (with LAF).

4 Observational data

We focus our analysis on the most important air pollutants for human health, namely NO_2, O_3 and $PM_{2.5}$. In this chapter, first the meteorological situation between 1 January and 30 June 2020 is analysed. Afterwards, observational air quality data at six selected measurement stations within the EEA network (https://www.eionet.europa.eu/countries/index) are presented and discussed.

4.1 Meteorological situation

During the lockdown period in spring 2020 large parts of the region of interest experienced exceptional weather that is assumed to have a strong influence on concentrations of some of the pollutants in focus.

The weather conditions during the first half of the year 2020 show strong variations across the months and a different character in the northern part of our model domain compared to more southern regions like the Po Valley. While in the North February was extremely wet and windy (south-westerly direction), the second half of March and April were very dry and sunny. Thus for meteorological reasons a comparison of pre-lockdown pollutant concentrations with those during the lockdown is fairly meaningless in assessing the effect of lockdown measures on the concentrations in the central and northern part of the region of interest.

To further analyse the weather regimes for the first half of 2020 the classification proposed by Hess and Brezowsky (1977) has been chosen (see also Bissolli and Dittmann (2001)). This classification identifies predominant synoptic regimes over Central Europe and defines 30 so called `Großwetterlagen´ (GWLs), which can be isolated by an objective method introduced by James (2007). The underlying data for this analysis were provided by the German Weather Service. The results of the GWL-classification can be found in Table A2

Pre-lockdown period

In February 2020, an unusually wet period occurred due to strong cyclonic activity in Central Europe. Westerly and North Westerly cyclonic regimes were observed on 76% of the days, whereas high pressure-type regimes were observed on only 24% of the days Thus, the shortwave downwelling irradiance in February 2020 is one of the lowest measured at the weather station Wettermast Hamburg (53°31' 09"N and 10°06'10"E) (https://wettermast.uni-hamburg.de) (Brümmer and Schultze, 2015) during the last 25 years (Figure A4), being representative for north western Europe. The accumulated precipitation for February at this weather station with an amount of more than 120 mm was exceptionally high compared to the last decades (Figure A4).

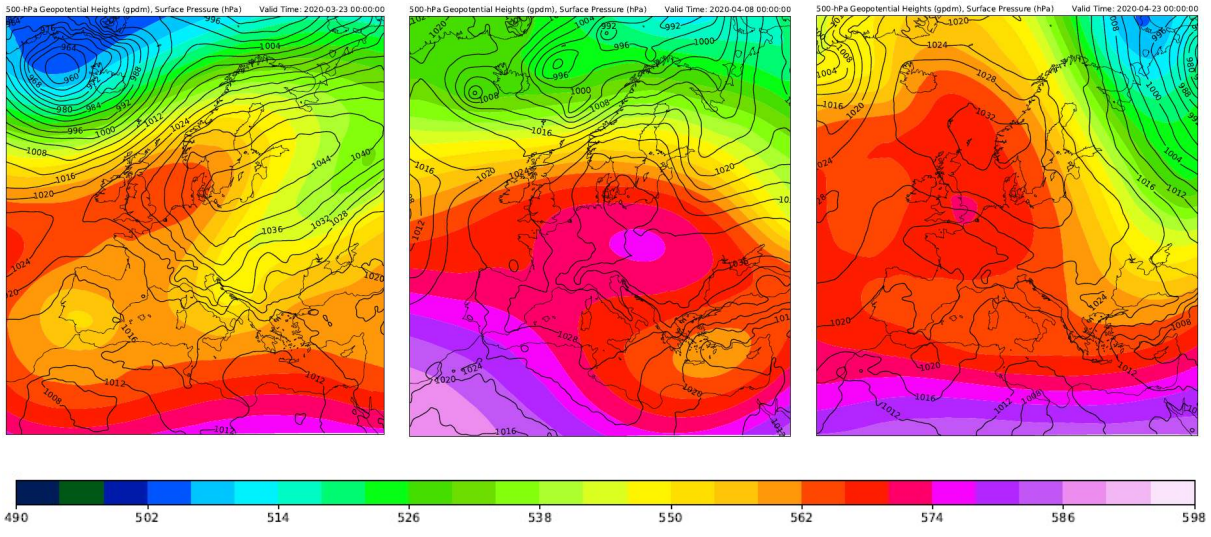

Figure 6: 500 hPa geopotential heights (in gpdm) and surface pressure (in hPa) for selected time segments in March and April 2020 according to the COSMO simulations. The geopotential heights are averaged over 4 days (21.03.-24.03; 6.04.-9.04., 21.04.-24.04. from left to right, respectively). Displayed surface pressure distributions are representative snap shots within those time segments.

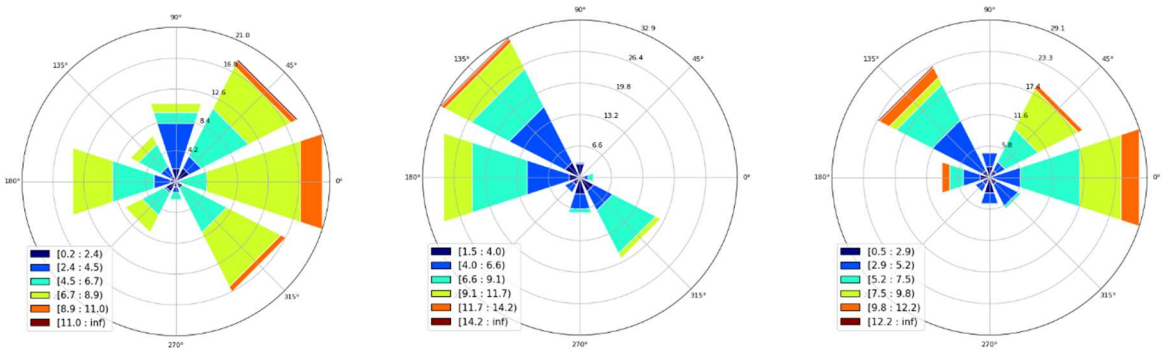

Figure 7: Wind roses derived from measurements of the weather station Wettermast Hamburg at an altitude of 110 m. Results for 3 periods covering about 15 days each are shown: 16.03. – 31.03.2020; 1.04.-15.04.2020; 16.04-30.04.2020, from left to right.

Main lockdown period

For the meteorological characterisation of the main lockdown period between mid of March and end of April we rely in addition to the GWL analysis on maps of the 500 hPa geopotential height and the surface pressure distribution. The underlying data were extracted from simulations with the COSMO-MERRA system, the same meteorological fields which have been used for the chemistry transport calculations with CMAQ displayed and discussed in the following chapters. In Fig. 6 a subset of those maps for 3 selected time periods is shown; the complete set of maps generated can be found in the appendix (Fig. A5). To characterise and quantify horizontal advection, wind roses derived from observations at the Wettermast Hamburg are displayed in Fig. 7. The wind data in each plot cover a time period of about 15 days. Measurements at an altitude of 110 m were chosen to better represent a larger area and eliminate parts of the surface influences on the wind.

In mid of March, the synoptic regime substantially changed over Europe. 'High pressure'-type GWLs became dominant, i.e. high ridges over Central Europe and high-pressure systems led to a typical atmospheric blocking of cyclones. The weather situation shows first a varying blocking in North- and Central Europe followed by a high pressure ridge reaching from the Azores to Scandinavia (Fig. 6, left), which changed to a high pressure ridge stretching from Iceland into Russia. In northern Germany the wind regime was dominated by a flow with mainly easterly components, which were relatively high wind speeds (Fig. 7, left). In southern Europe the situation, which was similar at the beginning of the period to that one in the North, changes starting about on the 23rd of March, an isolated trough formed leading to low pressure system activity. For March 28 and 29 dust transport from Asia and Northern Africa to the Po Valley was reported (Collivignarelli et al., 2020).

In the first half of April the weather in the north-eastern part of Central Europe was again quite variable, and in Southern Europe the cut-off from the northern regime could still be recognized. In the western part of Central Europe a ridge has established, which stretched towards the UK. Accordingly, winds in Northern Germany blew predominantly from westerly/north westerly directions. Later on, a ridge over entire Central Europe dominated the weather in the study domain (Fig. 6, middle), only the Eastern Mediterranean was still influenced by a cut-off trough. In the Po valley, according to measurements around Milan, the weather during the second half of March to April 10th was dry and very sunny with low to medium wind speeds (Collivignarelli et al., 2020). Towards the mid of April a high pressure bridge was established reaching from Iceland into Eastern Europe.

In the second half of April a high pressure system established over the British Isles attached to a ridge located over Central Europe leading to dry and sunny weather all over Europe. This condition was basically stable until April 25th, when a cyclonic flow took over, leading to more westerly winds over Central Europe, a situation which lasted until the first days of May. Winds in northern Germany switched over from easterly to more westerly directions this time (Fig. 7, right).

Overall, an exceptionally dry period occurred which started in the early lockdown period and continued until the end of April. The weather was characterized by very low cloud cover and record-breaking large amounts of solar irradiance (see the record at the Wettermast Hamburg in Fig. A4) and little precipitation. This exceptional weather period is also discussed by van Heerwaarden et al. (2021), who reported record breaking solar irradiation for the Netherlands.

Lockdown transition

In May 2020, atmospheric conditions were very different in Central Europe compared to the previous months. For instance, Germany was dominated by large amounts of rain in the South, sunny conditions in the West and dry but cloudy conditions in the East and North. Observed sunshine duration and solar irradiance corresponds approximately to average climatic conditions. In contrast, large parts of western Europe (Netherlands, Belgium, West Germany, UK) experienced sunny and dry weather throughout the entire May (van Heerwaarden et al., 2021). Finally, the large scale conditions in June turned out to favour long-lasting periods with dry and sunny weather conditions in northern Germany due to blocking conditions caused by high pressure systems located over Scandinavia. However, the more southerly regions were rather too wet in a climatological sense.

4.2 Concentrations of NO_2, O_3 and $PM_{2.5}$

The reduced emissions of pollutants during the lockdown periods should lead to changes in ambient concentrations of those substances and related secondary pollutants as ozone. Beside regional emissions advected pollutants and the meteorological conditions also determine local and regional concentrations. To assess changes in air quality and alterations in the behaviour and nature of concentration, time series observations at selected air quality measurement stations have been examined. The analysed stations have been selected in a way that they are geographically distributed over the study domain and represent different emission characteristics. The stations Radhuset in Malmö, Sweden, and Sternschanze in Hamburg, Germany, are classified as urban background stations, not directly influenced by traffic. Waldhof is a rural background station in northern Germany located about 60 km north of the city of Hannover. Vredepeel is a background station in a fairly populated part of the Netherlands situated in the triangle between the cities Nijmegen, Eindhoven and Venlo. The observatory Kosetice in the Czech Republic is located in the Moravian Highlands in an agricultural countryside about 80 km from south-east of Prague. To represent a region south of the Alps the Italian station San Rocco in Po-Valley about 30km east of Parma has been selected. With the exception of Kosetice, having an elevation of about 530m, the stations are situated below an altitude of 80m. To allow a comparison of the concentration measurements under different meteorological influences, time series of NO_2, O_3, and $PM_{2.5}$ for the years 2015 to 2020 have been examined. However, $PM_{2.5}$ was not available at the station San Rocco.

371

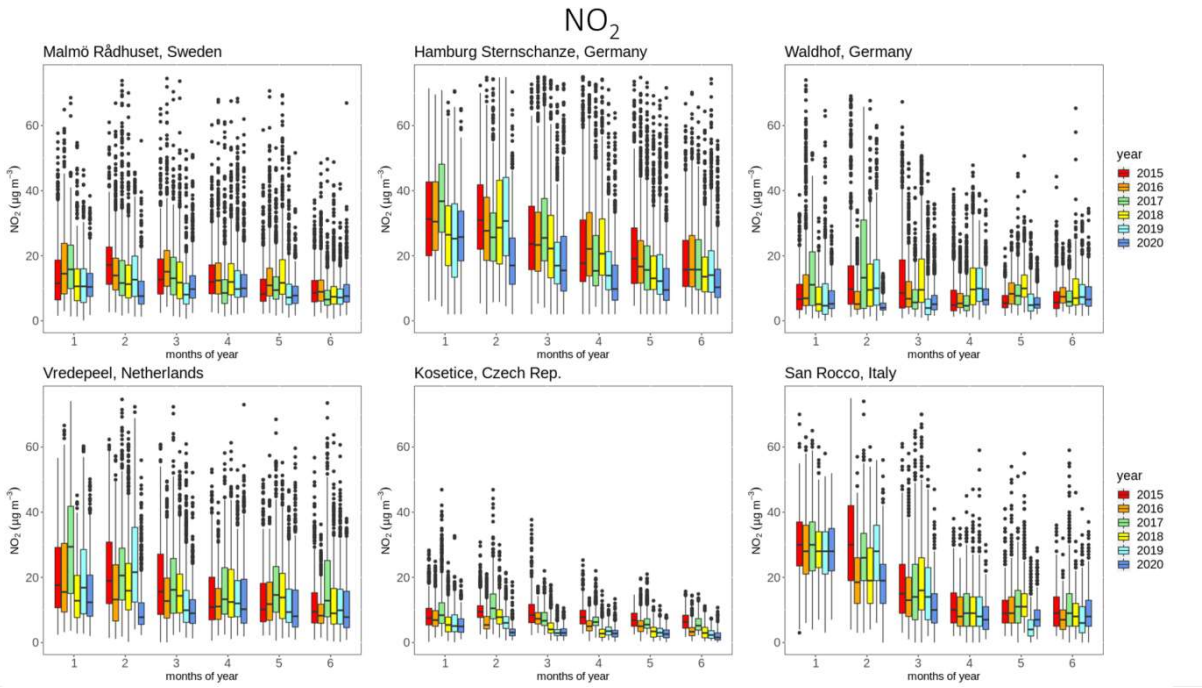
NO2
Malmö Rådhuset, Sweden
Hamburg Sternschanze, Germany
Waldhof, Germany
Vredepeel, Netherlands
Kosetice, Czech Rep.
San Rocco, Italy
NO2 (µg m-3)
months of year
year
2015
2016
2017
2018
2019
2020

372

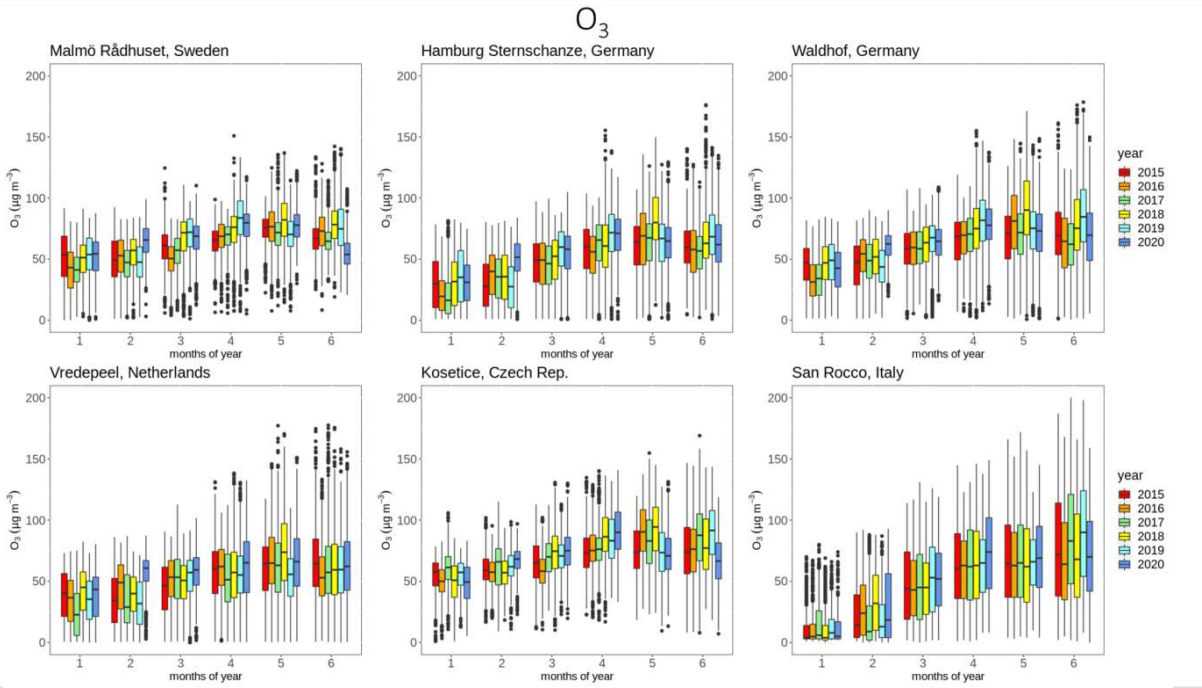
O3
Malmö Rådhuset, Sweden
Hamburg Sternschanze, Germany
Waldhof, Germany
Vredepeel, Netherlands
Kosetice, Czech Rep.
San Rocco, Italy
O3 (µg m-3)
months of year
year
2015
2016
2017
2018
2019
2020

373

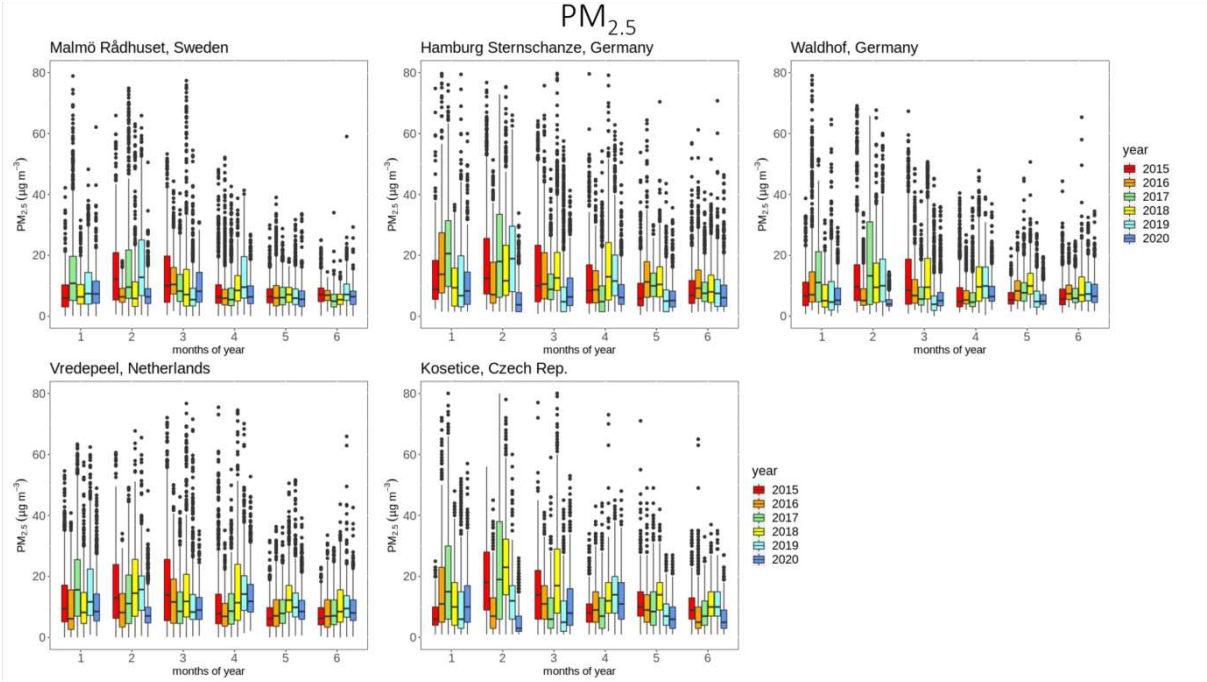

Fig. 8: Observed monthly concentrations of NO_2, O_3, and $PM_{2.5}$ at Waldhof (Germany), Vredepeel (The Netherlands), San Rocco (Italy), Kosetice (Czech Republic), Malmö (Sweden) and Hamburg (Germany). The median is displayed within the central boxes which span from the 25th percentile to the 75th percentile, called the interquartile range of the underlying frequency distributions. For NO_2 and $PM_{2.5}$ these distributions are based on hourly measurements at the different stations and for O_3 on daily 8 hour maximum values. The whiskers above and below the central boxes indicate the largest and the smallest value within 1.5 times the interquartile range, respectively. Dots denote values outside these ranges. $PM_{2.5}$ was not available at San Rocco.

The observational results for the selected stations for NO_2, O_3, and $PM_{2.5}$ are displayed in Fig. 8. For NO_2, at all stations, with the exception of Waldhof, an obvious trend from higher concentrations in the winter months to lower ones in spring in early summer can be seen. At Waldhof this trend is not that clear due to lower values in January for most of the years. As it can be expected, in urban (Malmö and Hamburg) or densely populated (Vredepeel and San Rocco) regions the NO_2 concentration are on a higher level. At most stations the NO_2 concentrations for March 2020, the month during which in all countries the lockdown measures started, are among the lowest ones compared to the previous years. For Hamburg, Vredepeel and Kosetice this also holds for the months April to June. An obvious feature, which appears at all stations except San Rocco is, that the February concentrations in 2020 are lower compared to the previous years, although no lockdown measures were taken in Europe in February. Presumably, meteorological conditions are responsible for these relatively low NO_2 concentrations. February 2020 was a month with steady westerly winds and longer periods of intense precipitation in Northern Europe. While strong winds cause rapid dilution of pollutants, steady precipitation has a cleaning effect due to dissolution of pollutants in cloud and rainwater and subsequent wash-out.

For O_3, at all stations and for all years the typical trend from low winter concentrations to higher concentrations in spring and early summer can be seen. During the lockdown month April the O_3 concentrations for the years 2018, 2019, 2020 were higher than in the previous years. During those years the radiation was rather intense in April, which favours the photochemical formation of ozone. At the rural stations Waldhof and Kosetice ozone concentrations in May and June 2020 were lower than in previous years. At the urban stations in Malmö and Hamburg the relative increase in O_3 concentrations over the 6 month period is lower compared to the more rural stations. This can be interpreted as a titration effect of O_3 by reactions with NO, which has significant sources in

urban areas. In general, the observations of O_3 maxima do not provide any indication of significant effects related to lockdown emission changes in 2020.

$PM_{2.5}$ concentrations also show no clear signal that would allow to relate concentrations to lockdown emission reductions. Slightly higher concentrations and variability can be observed in winter compared to summer at all stations. This can be related to the fact that very high PM concentrations appear in winter, only, when emissions are high and atmospheric mixing is suppressed, e.g. during high pressure situations with advection of cold air. Similar to the NO_2 concentrations, rainy and windy weather in February 2020 leads to low $PM_{2.5}$ concentrations at all stations.

4.3 Model results at measurement stations

In order to judge the quality of the model results, simulated concentrations were compared to observations at selected stations, including some of those presented above. Fig. 9 exemplarily shows the comparison at Vredepeel, Table 1 contains statistical values for NO_2 and O_3 at 11 stations and for $PM_{2.5}$ at 4 stations in Europe.

Modelled NO_2 concentrations are typically lower than the observed values, in particular, the model shows a stronger downward trend of the concentrations in spring than observed. This pattern is reversed for ozone, where the modelled 8h max concentrations are typically too high with better agreement in spring compared to winter. $PM_{2.5}$ is underestimated on average, but only at 2 out of 4 stations. Here, the agreement is typically better in winter compared to spring. As average for all selected stations, the model bias for NO_2 is -17%, for O_3 it is +21% and for $PM_{2.5}$ it is -5%. The temporal correlation (R^2) based on daily mean values varies between 0.42 and 0.74 for NO_2, between 0.07 and 0.75 for O_3 and between 0.21 and 0.62 for $PM_{2.5}$. Details are given in Table 1.

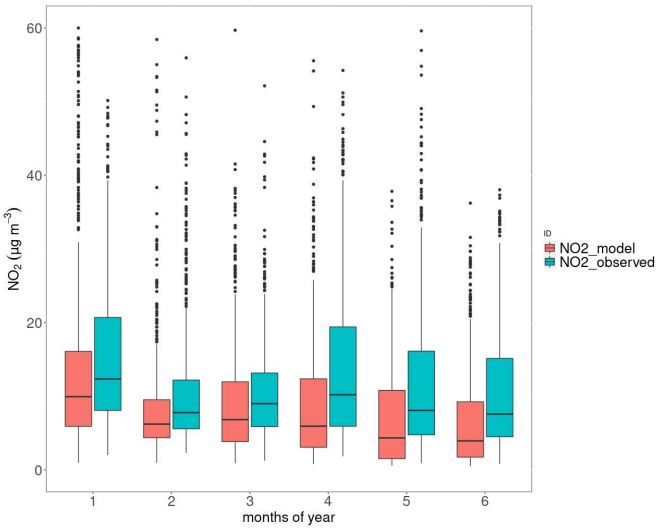

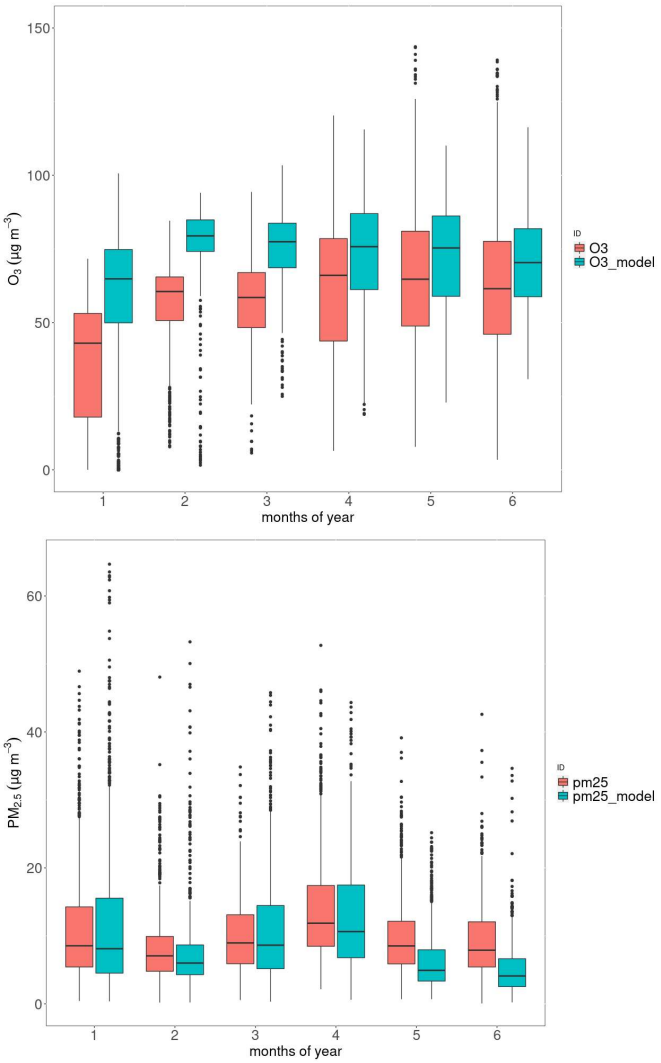

Fig. 9: Comparison between model results (green) and observations (red) at Vredepeel, Netherlands. Top: NO_2, middle: O_3, bottom: $PM_{2.5}$. All concentrations are given in µg/m³, box plots show medians, 25% and 75% quartiles and whiskers representing 1.5 times the interquartile range. Values that fall outside the range of the whiskers are given as dots.

Table 1: Statistical evaluation of a comparison between observations of NO_2 at selected background stations of the EEA network with CMAQ model results between 1 Jan 2020 and 30 June 2020

Station	Observed [µg/m³]	Modelled (COV case) [µg/m³]	Bias (model- obs) [µg/m³]	Correlation
NO_2 concentrations 1 Jan 2020 – 30 June 2020				
Risoe, DK	4.7	5.7	1.0	0.46
Waldhof, DE	5.0	3.8	-1.2	0.63
Zingst, DE	4.4	2.9	-1.5	0.63

Neuglobsow, DE	2.9	2.6	-0.3	0.66
Vredepeel, NL	12.4	10.2	-2.2	0.64
De Zilk, NL	11.4	12.8	1.4	0.51
Kosetice, CZ	3.4	3.0	-0.3	0.42
San Rocco, IT	13.5	9.2	-4.3	0.74
Besenzone, IT	15.8	11.9	-3.9	0.71
Casirate d'adda, IT	19.4	15.9	-3.5	0.71
Paray le Fresil, FR	3.1	2.1	-1.0	0.54
O_3 concentrations 1 Jan 2020 – 30 June 2020				
Risoe, DK	71.2	75.7	4.5	0.07
Waldhof, DE	63.6	74.5	10.9	0.25
Zingst, DE	70.6	79.7	9.1	0.23
Neuglobsow, DE	62.8	74.8	12.0	0.16
Vredepeel, NL	56.8	70.5	13.7	0.55
De Zilk, NL	63.1	70.6	7.5	0.34
Kosetice, CZ	70.0	78.6	8.6	0.21
San Rocco, IT	54.7	73.4	18.7	0.68
Besenzone, IT	49.5	69.3	19.8	0.59
Casirate d'adda, IT	56.3	74.0	17.7	0.75
Paray le Fresil, FR	58.6	77.2	18.6	0.43
$PM_{2.5}$ concentrations 1 Jan 2020 – 30 June 2020				
Waldhof, DE	6.8	7.3	0.5	0.21
Vredepeel, NL	10.6	9.2	-1.4	0.57
De Zilk, NL	6.8	7.8	1.0	0.44

Kosetice, CZ	9.3	7.8	-1.5	0.62

5 COVID-19 lockdown effects

Effects of the lockdown measures on emissions were discussed in section 3. Now, CMAQ model results are evaluated for the COV and the noCOV case during the lockdown phase. Meteorological impacts are discussed through comparisons of CMAQ model results that were derived with meteorological data for the years 2016 and 2018.

5.1 CMAQ results for Central Europe

Differences between the CMAQ results for 2020 for the COV and the noCOV case reveal the impact of the lockdown emission reductions on air pollutant concentrations. The magnitude of the concentration changes varies considerably in time and space. Here, we focus our evaluation on the period with the highest emissions reductions between 16 and 31 March 2020. During this time the most widely spread and temporally stable emission reductions took place in Europe. Differences among weekdays and weekends and, to a limited extent, also among different weather situations are averaged out by investigating a half-month-period. However, changing effects over time are also discussed.

NO_2 concentrations

Fig. 10 shows maps of the modelled average NO_2 concentrations in Central Europe between 16 and 31 March for the case without lockdown measures (noCOV) together with the absolute and relative concentration reductions caused by the lockdown. The NO_2 concentrations for the noCOV case in central Europe show the typical pattern with highest concentrations in densely populated areas like England, Belgium, The Netherlands and western Germany as well as northern Italy (Fig 10a). Average concentrations range between 5 and 10 µg/m³. Reductions in NO_2 concentrations caused by the lockdown are highest in the same regions, also reaching several µg/m³. Relative reductions are highest in France, Belgium, Italy, and Austria, reaching more than 40% on average. Germany, The Netherlands, UK, southern Sweden and the Czech Republic show lower reductions between 15% and 30%. In the following weeks, NO_2 concentrations stayed more or less on the same level in most parts of Europe, but the lockdown effects decreased slightly as it could be expected from the emission changes. Overall, relative concentration reductions were most significant in England, France, Belgium and Italy, as it was seen for the second half of March. Maps for relative reductions due to the lockdown for six half-month periods between 1 March 2020 and 31 May 2020 are given in the appendix (Fig A6).

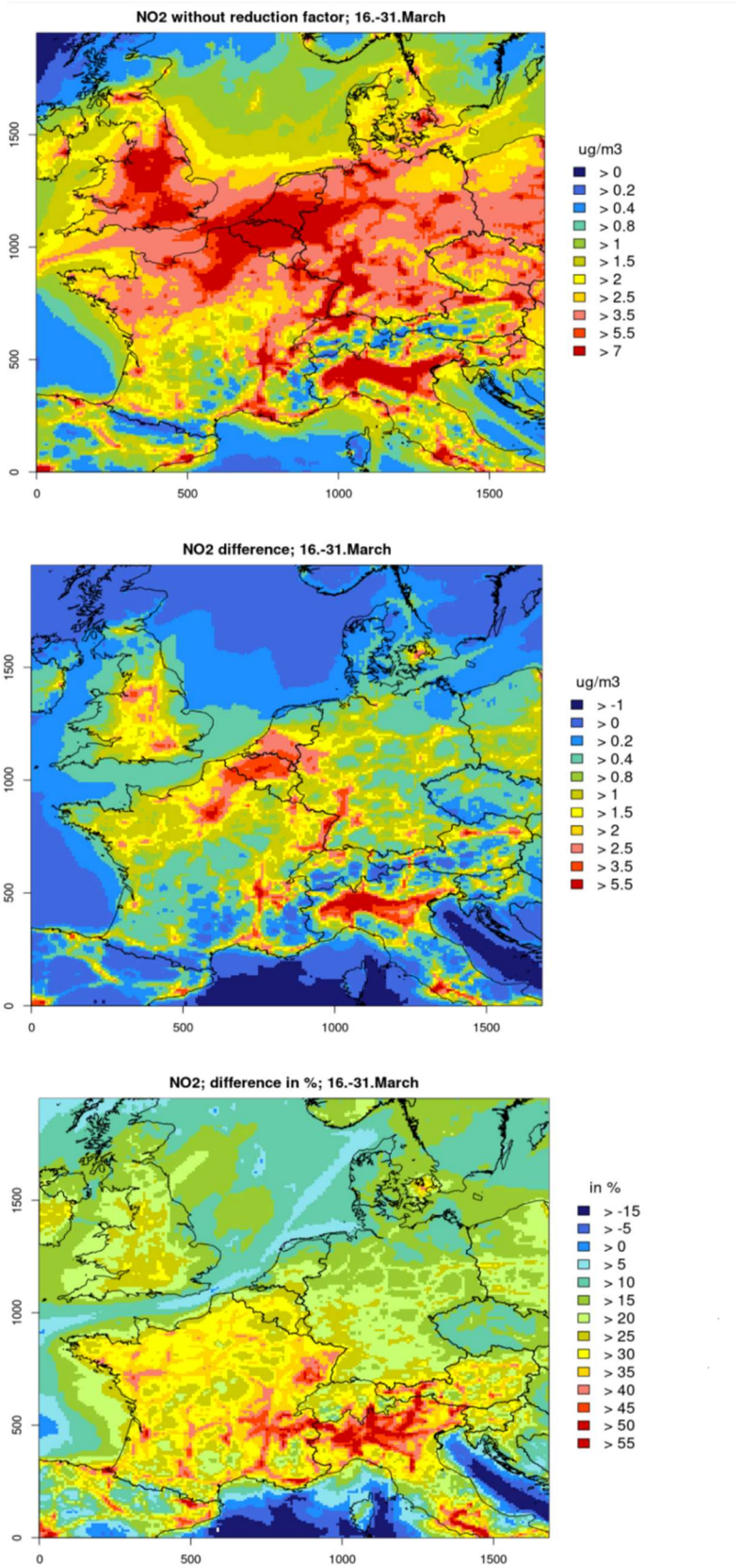

Figure 10: CMAQ results for NO_2 concentrations in Central Europe between 16 and 31 March 2020. Top: Concentrations without lockdown measures (noCOV run). Middle: Absolute concentration reductions due to lockdown measures (noCOV – COV run). Bottom: Relative concentration reductions due to lockdown measures (noCOV – COV run); positive values for absolute and relative differences denote high reductions.

464 **O_3 concentrations**

465 It can be expected that reduced NO_x emissions are also reflected in modified O_3 concentrations with lower values
466 in all regions that are NO_x-limited. However, for the second half of March increased O_3 concentrations between
467 1 and 8 µg/m³ were modelled in the COV case for northern Central Europe and the Po valley (Fig. 11). Because
468 these are the regions with the highest NO_x emissions in Europe, they were most likely VOC-limited during this
469 first lockdown period and O_3 titration with NO was reduced when NO_x emissions were reduced. Most of the
470 southern parts of the modelling domain exhibited a decrease in ozone of 1-2 µg/m³ on average caused by the
471 lockdown and the reduced NO_x emissions. In the following weeks, areas with increased ozone turned smaller
472 week by week and were limited to large cities and the most densely populated areas, see Fig 12 for the first half
473 of April and the first half of May. Most regions in Europe turned into NO_x-limited areas in spring 2020, resulting
474 in lower ozone concentrations of 1-2 µg/m³ (about 2-4% change) caused by the emission changes during the
475 lockdown (Fig. A7).

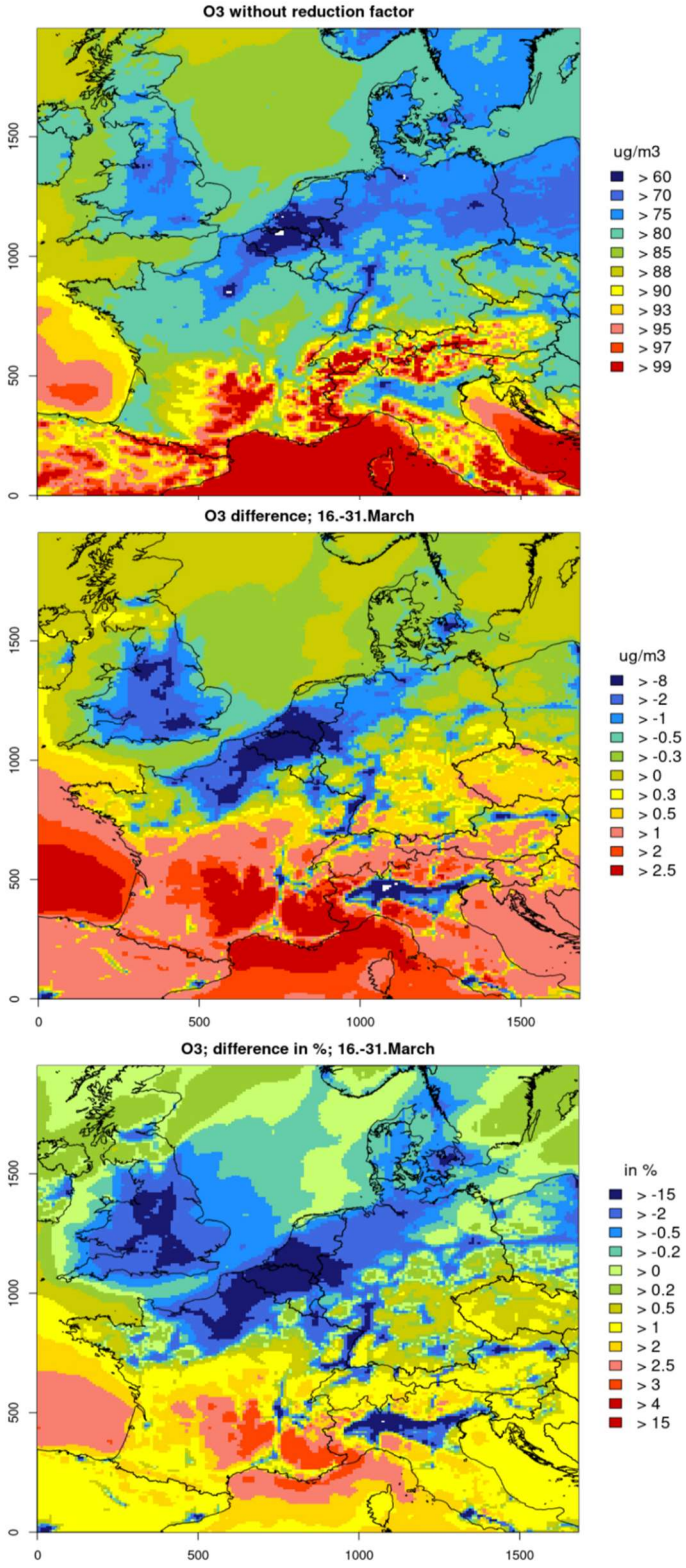

Fig. 11: CMAQ results for O_3 concentrations in Central Europe between 16 and 31 March 2020. Top: Concentrations without lockdown measures (noCOV run). Middle: Absolute concentration reductions due to lockdown measures (noCOV – COV run); positive values denote high reductions. Bottom: Relative concentration reductions due to lockdown measures (noCOV – COV run); positive values denote reductions, negative values denote increases.

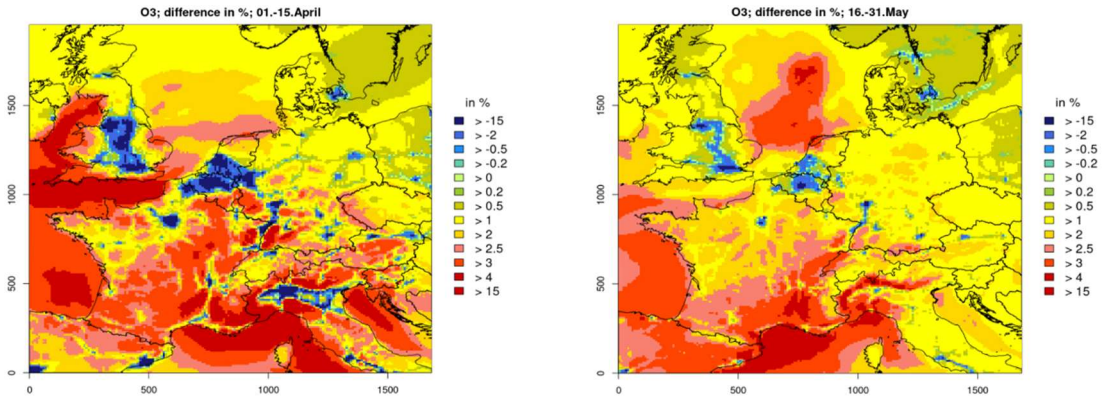

Fig. 12: CMAQ results for changes in O_3 concentrations due to lockdown measures in Central Europe between 1 and 15 April 2020 (left) and 16-31 May 2020 (right). Positive values denote concentration reductions, negative values denote concentration increases.

$PM_{2.5}$ concentrations

Simulated $PM_{2.5}$ concentrations in the second half of March 2020 for the noCOV case show relatively high concentrations between 12 and 15 µg/m³ in large parts of Central Europe and the Po valley while the UK, Denmark and Northern Germany exhibited concentrations below 10 µg/m³ (see Fig. 13, top). The lockdown emission reductions lead to concentration reductions between 1 and 3 µg/m³ in those regions with higher concentrations and values below 1 µg/m³ in the north western part of the domain. Relative concentration decreases were most significant in France and northern Italy with values up to 20% while in the rest of the domain 6-10% lower $PM_{2.5}$ was simulated. In the following weeks, $PM_{2.5}$ concentrations were typically reduced by 10-20% because of the lockdown measures in most parts of Central Europe. Somewhat lower values were found in the northern and southern parts of the domain. The reduction in $PM_{2.5}$ concentrations decreased to 6-12% in the second half of May (see Fig. A8 in the supplement).

An investigation of the chemical components of the modelled $PM_{2.5}$ concentrations for the noCOV case reveals that about 2/3 consists of the inorganic components nitrate (NO_3^-), sulphate (SO_4^-) and ammonium (NH_4^+). The lockdown measures caused large reductions in NO_x emissions. Consequently, nitrate was reduced by more than 24% in large parts of France and northern Italy between mid of March and end of April, see Fig. A9 in the appendix. The reduction was usually somewhat lower in other parts of the domain. Particulate nitrate is mostly bound to ammonium, however, the model results show a lower relative reduction of the ammonium concentrations compared to nitrate. It is only in the order of 8-20% at maximum (Fig. A10). This is because ammonium is preferably bound to sulphate in atmospheric aerosols and sulphate concentrations even increased by a few percent as a consequence of the lockdown measures (Fig. A11). This can be explained by the large reduction in the formation of particulate nitrate in the COV case. Less nitrate means less ammonium which is then available as gaseous ammonia. This may lead to the formation of additional ammonium sulphate in areas where gaseous sulphuric acid is available.

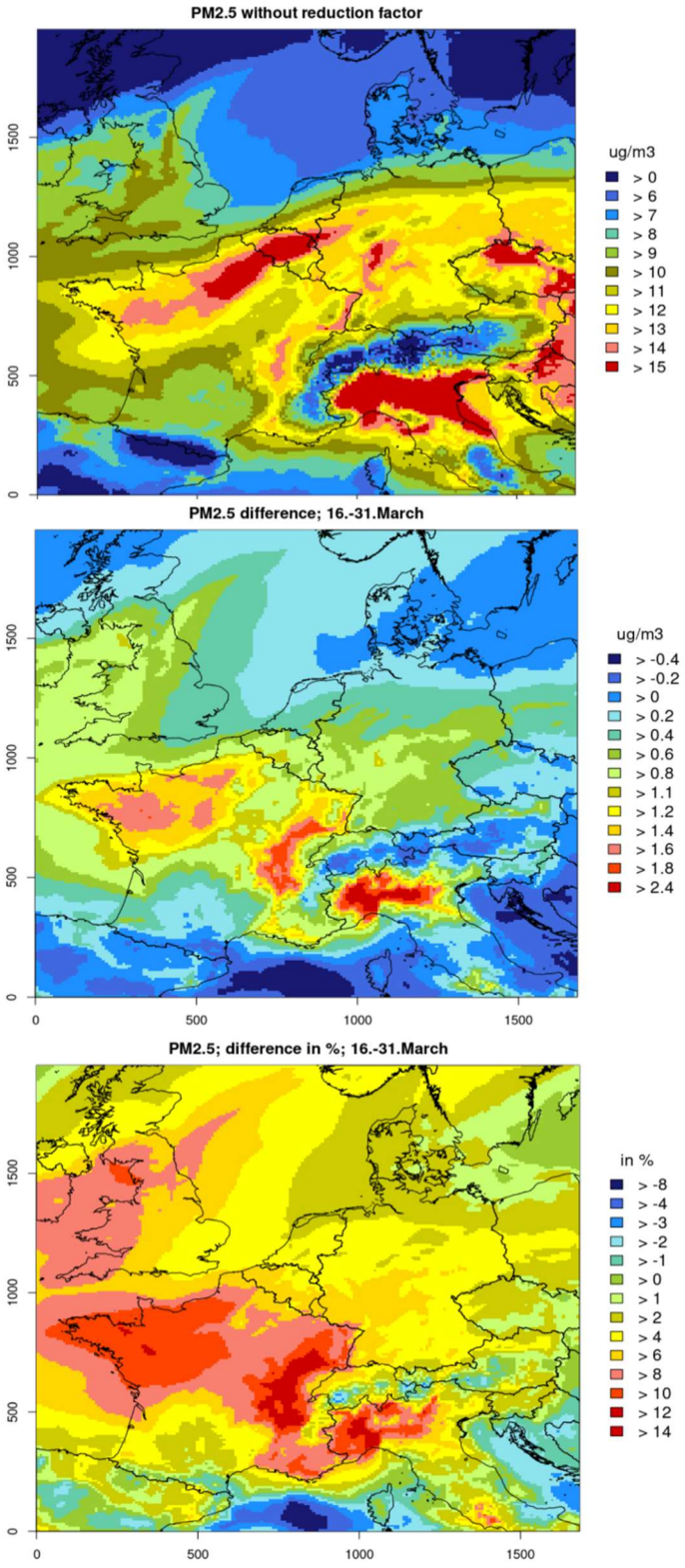

Fig. 13: CMAQ results for $PM_{2.5}$ concentrations in Central Europe between 16 and 31 March 2020. Top: Concentrations without lockdown measures (noCOV run).Middle: Absolute concentration reductions due to lockdown measures (noCOV – COV run); positive values denote reductions. Bottom: Relative concentration reductions due to lockdown measures (noCOV – COV run); positive values denote reductions.

Temporal development of concentration changes

The detailed temporal development of the effect of lockdown emission reductions on atmospheric concentrations of NO_2, O_3 and $PM_{2.5}$ is followed at selected measurement stations. Figure 14 shows the modelled differences between the noCOV and the COV model runs at Waldhof, Vredepeel, and San Rocco. Lockdown emission reductions lead to reduced concentrations of NO_2 and $PM_{2.5}$ at all stations, however, the amount varies considerably in time and by station. At Waldhof, only very small changes are simulated. At Vredepeel, NO_2 is significantly reduced (by more than 10 µg/m³ on individual days) $PM_{2.5}$ shows only small reductions. At San Rocco, both, NO_2 and $PM_{2.5}$ are reduced by several µg/m³ until the end of April. In May and June, lockdown effects on the concentrations get much smaller, also at Vredepeel and San Rocco.

O_3 shows higher values despite the emission reductions until mid of April at Vredepeel and San Rocco. This is because these stations are in VOC-limited areas at that time, where NOx emission reductions lead to decreased O_3 titration. This pattern changes towards end of April and in the following O_3 is decreased on most of the days at all stations as a consequence of lower NOx emissions. This effect remains variable at Vredepeel, a station close to the region with highest NOx emissions in Europe. At Waldhof, O_3 reductions are observed between beginning of April and end of June. On average between 16 March and 30 June, O_3 is only decreased by 0.6 µg/m³ (< 1%) at Vredepeel. At Waldhof and San Rocco, the reductions are 1.2 µg/m³ (1.6%) and 1.5 µg/m³ (1.9%), respectively.

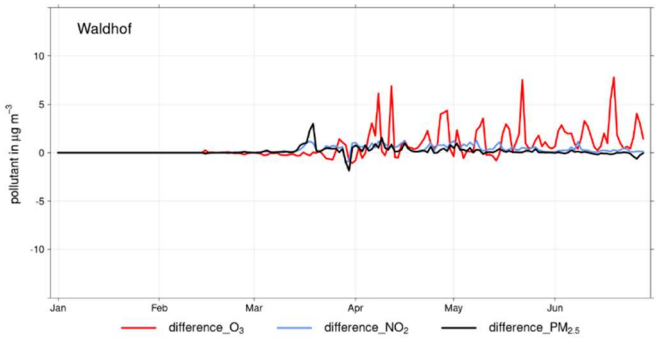

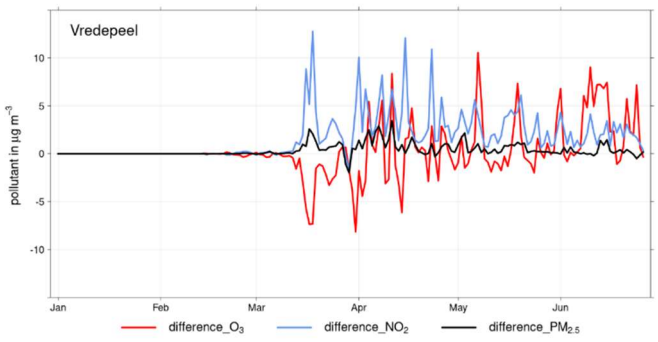

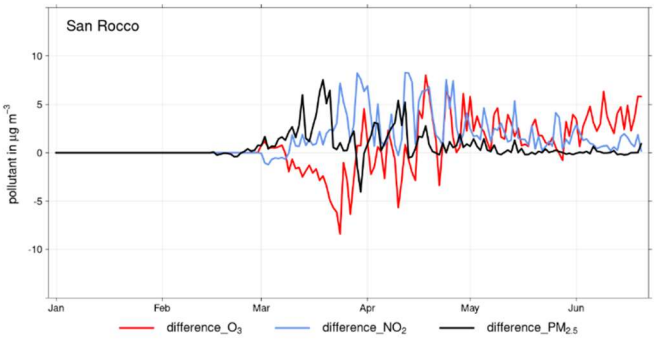

Fig. 14: Temporal development of the differences in the simulated concentrations of O_3 (red), NO_2 (blue) and $PM_{2.5}$ (black) in Waldhof (top), Vredepeel (middle) and San Rocco (bottom) between 1 January and 30 June 2020.

5.2 Impact of meteorological conditions

For investigating the effects of the exceptional meteorological situation on the concentration reductions in March and April 2020, additional CMAQ model simulations were performed. Meteorological data simulated with COSMO-CLM for the first six months in 2016 and 2018 was used as input data, together with the 2020 emissions for both the COV and the noCOV case. Biogenic emissions were also kept the same for the 2016 and 2018 runs in order to investigate effects of meteorological conditions only. These additional years were selected to cover a span of weather situations during the lockdown phase. The selected years were different, but represent not in any sense an extreme situation. They were chosen from the time span 2015 to 2019, since for these years model data generated using the same advanced model settings (model version and reanalysis data) is available. The results show the concentration and the changes caused by the lockdown measures as they would have happened under different meteorological conditions.

Fig.15, top, shows the NO_2 concentration changes for 2020 relative to 2018 and 2016 caused by meteorological conditions, only, for the period between 16 March and 30 April. No emission changes because of the lockdown were assumed for this investigation. Meteorological conditions in 2020 caused between 20% and more than 30% lower NO_2 concentrations in large areas of the north eastern model domain (The Netherlands, northern Germany, Denmark and southern Sweden) compared to 2018, even without any lockdown measures. On the other hand, in western UK, Belgium, northern France, and the Czech Republic, meteorological conditions led to 20% to more than 30% higher NO_2 concentrations. The picture is similar when compared to 2016, in particular in the western part of the model domain, but the area with lower NO_2 concentrations in 2020 compared to 2016 does not include the North Sea and Denmark.

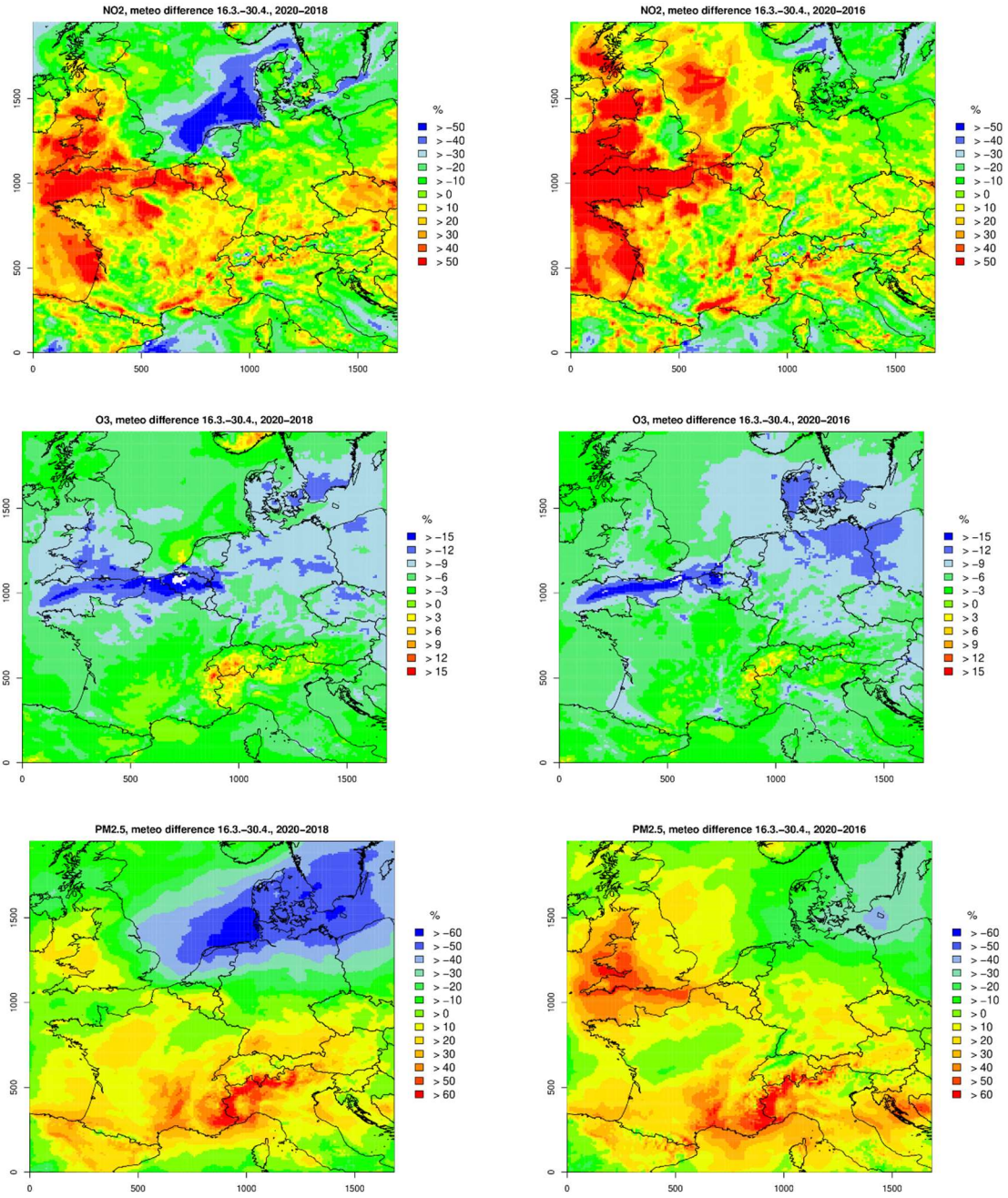

Fig. 15: Relative concentration changes due to meteorological conditions in Central Europe between 16 March and 30 April simulated with CMAQ for NO_2 (top), O_3 (middle) and $PM_{2.5}$ (bottom): The changes are represented as relative numbers for 2020 compared to 2018 (left) and 2016 (right). Positive values denote higher concentrations in 2020 relative to the previous year. Be aware of the different scales for each pollutant.

Average ozone concentrations between 16 March and 30 April 2020 were relatively low in almost entire Central Europe when compared to a situation with meteorological conditions as in 2018 and 2016 (see Fig. 15, middle). Differences are in the order of 10-15% in the northern part of the model domain and between 2 and 6% in the southern part. Only in few spots in northern Italy and southern Switzerland, the meteorological situation in 2020 favoured ozone formation compared to 2016 and 2018.

The picture is more mixed for $PM_{2.5}$ with considerably lower concentrations in 2020 compared to 2016 and 2018, particularly in northern Germany and Poland, i.e. in the north eastern part of the domain (Fig. 15, bottom). Relative differences reach more than 50% between 2020 and 2018 in the German Bight. Compared to 2018, $PM_{2.5}$

concentrations were also low in the western UK in 2020. In almost entire France and in northern Italy, $PM_{2.5}$ concentrations were relatively high in 2020 compared to 2016 and 2018, differences again reach more than 50% but with opposite sign.

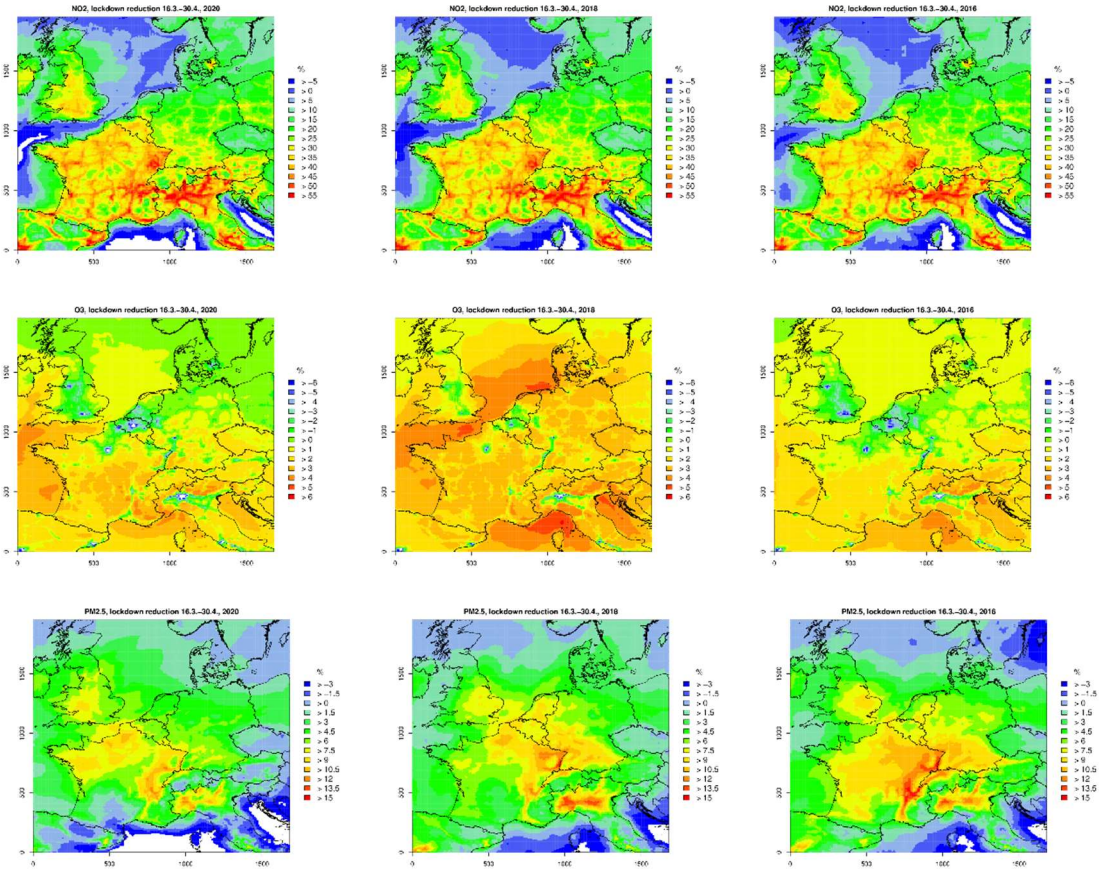

Fig. 16: Relative concentration reductions due to lockdown measures (noCOV – COV run) in Central Europe between 16 March and 30 April simulated with CMAQ for NO_2 (top), O_3 (middle) and $PM_{2.5}$ (bottom) and three different meteorological input data sets. Left: 2020, Middle: 2018, Right: 2016. Positive values denote concentration reductions caused by the lockdown emission changes. Be aware of the different scales for each pollutant.

The meteorological situation also affects the concentration changes caused by the lockdown, but this differs considerably among the pollutants. Fig 16 shows the lockdown emission reduction effects on the average concentrations for the main lockdown period from 16 March to 30 April. In most parts of Central Europe the variation for NO_2 is rather small (plus/minus approx. 5%). For ozone, on the other hand, effects of the lockdown are quite different among the three selected meteorological years. For 2020 meteorological conditions, relatively large areas in Northern Central Europe show a slight increase in ozone (green and blue areas in Fig. 16, middle row). These areas would have been smaller with 2016 meteorological conditions and limited to the most densely populated areas for 2018 meteorological conditions. Lockdown effects on $PM_{2.5}$ would have been more significant under meteorological conditions of the years 2016 and 2018 in almost the entire model domain (Fig. 16, bottom row). Particularly in northern Italy and south eastern France, changes in $PM_{2.5}$ caused by the lockdown could be more than 10%, a value that was rarely reached during the real lockdown in 2020.

6 Discussion

6.1 Emission estimates

Emissions for 2020 were estimated based on data for 2016 and extrapolation factors that resemble the temporal development of total sectoral emissions during 3 years before 2016. This method leads to emission corrections that are typically on the order of 10% but may be up to 40%. This method bears some uncertainties, however, in countries that have a high share in the total emissions in Central Europe, emission trends were rather stable during the last 20 years. Good agreement between observed and modelled concentrations during the weeks before the lockdown gives confidence in the method.

Estimates for lockdown emission reductions also include several sources of uncertainty. Reduction of NO_x emissions from traffic have the largest share in the emission reductions. In this approach, the LAFs applied are based on google mobility data that resembles all traffic activities, regardless of their real emissions. I.e. no distinction between trucks and small private cars is made and it seems likely that traffic related to transporting goods was less reduced than private and commuter traffic. Therefore, emission reductions in traffic might be overestimated. On the other hand, possible emission increases for residential heating that are related to more people working from home were considered to be small and neglected here. Small changes in other sectors like off-road machinery that might have taken place weren't considered, either.

The cubic spline interpolation, applied to derive daily LAFs from monthly statistical data, enables to represent the mean of each month correctly while giving an assumption on the daily values with a rather smooth curve. This assumption does not necessarily represent the real daily conditions as extrema in the interpolation always occur at the start or in the middle of the month, which might not be the case in reality. However, it is an improvement compared to using monthly averages for each day of the month, as in this case, extreme jumps can occur at the transition to the next month that author's assume to be more unrealistic. In addition it might resemble the rapid emission reductions mid of March better than a monthly value.

Similar approaches to calculate lockdown adjustment factors were followed by Doumbia et al. (2021) and Guevara et al. (2021). Both estimate that decreases in NO_x emissions in Central Europe taking all sectors together were around 30% in April 2020, which is in very good agreement with the numbers that were derived in this study. This study focuses on Europe and calculates LAFs for each country in a detailed way based on the same data source for each sector. Doumbia et al. (2021) use information from other sources than here (e.g. for aviation, shipping and industry) which are partly less well resolved in time, however, they provide adjustment factors for the entire world. Also emissions from residential areas were treated differently. While Doumbia et al. (2021) see an emission increase, they remained unchanged in this study. The reasoning behind this is that the heating demand is most likely not significantly modified when more people stay at home compared to the case when they go to work. This assumption is in agreement with earlier estimates by Le Quéré et al. (2020) who calculated only small emission increases in the sector Residential. Compared to Guevara et al. (2021), the time period considered in this study is longer and reaches till the end of June 2020.

6.2 CTM results

Chemistry transport model simulations are always connected with uncertainties, stemming from unknown or incorrectly represented processes or input data. The former includes chemical reactions, transport and deposition processes, the latter includes emission data and meteorological fields. Nevertheless, the model is able to reproduce

observed concentration levels and their spatiotemporal variation. The agreement between modelled and observed concentrations (see section 4.3) is in a range that is typical for regional CTMs (see e.g. Solazzo et al. (2012)). The deviations from the observed values can be interpreted as relative uncertainties in the modelled lockdown effects. During the lockdown between March and June, deviations between modelled and observed concentrations are often higher than the changes caused by the lockdown. Therefore, the results cannot be used to judge how accurate the estimated emission reductions are. It should be noted also that the simulations for 2016 and 2018 do not resemble the real situation during these years, because all emissions and chemical boundary conditions were for 2020.

NO_2 concentrations

During the six weeks of the most stringent lockdown measures in Central Europe (16 March to 30 April), emission reductions caused NO_2 concentrations reductions between 15% and more than 50%. This is in good agreement with other studies (Velders et al., 2021;Menut et al., 2020;Gaubert et al., 2021) and also close to what was estimated from satellite observations. Bauwens et al. (2020) report columnar NO_2 reductions of approx. 20% around Hamburg, Frankfurt and Brussels, 28% for the area around Paris and 33 – 38% for Northern Italy. These reductions are almost independent of the meteorological situation, as can be seen in Fig 16 (top row). Differences in modelled NO_2 concentrations between 2020 and 2016 or 2018 show variations of more than 30%, but they are fluctuating in both directions on small spatial scales (see Fig. 15, top row). Larger areas with systematic differences are mainly found over sea and in areas with relatively low average concentrations, like in the western UK. It can be concluded that the NO_2 concentration reductions during the lockdown were dominated by the emission reductions and not very much by the meteorological situation. This is in agreement with the fact that NO_2 concentrations are spatially closely connected to the emission sources. NO_2 is quickly formed from NO after the latter was emitted into the atmosphere. It will then react further to form O_3 at daytime. Compared to O_3 and secondary PM, NO_2 is a rather short-lived gas with high spatial gradients and a clear annual cycle. However, as the situation in February 2020 shows, very unusual meteorological conditions can also cause large deviations from expected concentrations.

O_3 concentrations

Ozone concentrations depend more strongly on weather conditions and on emissions of other precursors like VOCs. Therefore, meteorological variations from year to year might have a much stronger influence on average concentrations than the emission reductions during the lockdown. The six-weeks-average ozone concentrations vary by +/- 15% between 2020 and 2016 or 2018 (Fig 15, middle row) while the lockdown effects are mostly in the range of +/- 5% (Fig 16, middle row), except in densely populated areas. Weather conditions between 16 March and 30 April 2020 favoured relatively lower ozone concentrations in most parts of Central Europe when compared to 2016 and 2018. In the simulations, only areas in the western Alpine region show higher ozone in 2020 (Fig 15, middle row). First of all, this is surprising because 2020 was comparably sunny and dry, which should favour ozone formation. The latter was also stated by Deroubaix et al. (2021) and Gaubert et al. (2021) in their studies about the COVID19-lockdown effects on air quality. However, advection of relatively clean air from Scandinavia into the North Eastern part of the model domain led to lower ozone concentrations particularly in the second half of April. A comparison of the meteorological effects on NO_2 and O_3 in Fig 15 also shows that NO_2

was relatively high and O_3 relatively low in 2020 in the English Channel, in south western UK and Belgium. The high pressure situation with relatively low wind speeds in 2020 resulted in efficient ozone destruction at night in areas with high NO emissions.

Lockdown effects on ozone might differ in sign under different meteorological conditions, as can be seen in Fig 16. The emission reductions caused relative ozone increases in urban areas and throughout the northern part of the model domain, because these areas are VOC-limited regions. This was also reported by Menut et al. (2020) and Mertens et al. (2021). The effect is most pronounced in the second half of March and then decreases over time when VOC emissions, in particular from natural sources, increase (Fig. A7). In northern Central Europe the small effects on ozone are connected with advection of clean air from north east. For most parts of Central Europe, O_3 concentrations were decreased by lockdown measures. About 2-4% O_3 concentration reductions in most parts of Central Europe could have been expected with 2018 meteorological fields, when solar radiation was lower but more southerly winds prevailed in northern Central Europe. On the other hand, with 2016 meteorological conditions ozone changes would show similar patterns as 2020. Ozone chemistry depends on radiation, precipitation, atmospheric mixing and the availability of precursors in a complex way. The response of ozone concentrations to emission changes is therefore not straightforward to predict. Also long range transport, which was neglected here, may play role (see also Deroubaix et al. (2021) and Mertens et al. (2021)).

$PM_{2.5}$ concentrations

$PM_{2.5}$ is another secondary pollutant that depends strongly on weather conditions, but emission reductions will primarily lead to concentration reductions (see Figures 13 and 14). However, the strength of this effect might also vary considerably with meteorological conditions. Fig 15 (bottom row) shows that the main lockdown period in 2020 was favourable for $PM_{2.5}$ formation in most parts of Central Europe, with often 20% to 50% higher $PM_{2.5}$ concentrations compared to other meteorological situations. An exception is the north eastern part of the model domain, where the meteorological situation in 2020 led to much lower $PM_{2.5}$ concentrations compared to 2018 (more than 50% lower) and 2016 (20-40% lower). Similar to the situation for ozone, this is connected to the easterly and north easterly winds and the advection of clean air. Consequently, lockdown emission reductions had only very minor effects on $PM_{2.5}$ concentrations in 2020 in southern Sweden, Denmark, Poland and northern Germany.

Among the $PM_{2.5}$ components, particle bound nitrate is reduced strongest (Fig. A9-A11). Sulphate might even increase in some areas where ammonia becomes available when ammonium nitrate aerosol concentrations are reduced. Small amounts of additional ammonium sulphate can then be formed. Reduced VOC emissions are likely to cause also a decrease in secondary organic aerosol (SOA) formation, as proposed by Gaubert et al. (2021). Given the uncertainties in SOA formation mechanisms in regional CTMs (Bessagnet et al., 2016), lockdown effects on SOA were not investigated in this study.

Higher $PM_{2.5}$ reductions would have been observed in most parts of Europe with 2016 and 2018 meteorological conditions. This can be interpreted in a way that the main lockdown period in 2020 was favourable for $PM_{2.5}$ formation in large parts of Europe leading to smaller relative $PM_{2.5}$ concentration reductions, given that the emission changes are the same.

Summarized, it can be said that the effects of lockdown emission reductions depend strongly on the meteorological situation and that concentration changes because of weather conditions might be stronger than those of large emission changes during a six weeks period in spring. However, this mainly holds for the secondary pollutants O_3 and $PM_{2.5}$, while the effects on NO_2 concentrations are less pronounced. Particularly changes in O_3 concentrations are difficult to predict because of the complex emission-chemistry-meteorology interactions.

7 Conclusions

Lockdown emission reductions in spring 2020 in Central Europe were significant, in particular those in traffic. Other sectors, like shipping, might be of regional importance, but emission changes for this sector are less certain. Aviation shows the largest relative reduction among the emission sectors considered, however the contribution to the total emissions reductions is small because of its low share in total NO_x emissions. Consequently, strongest lockdown emissions reductions are seen for cities. The period with largely reduced emissions was limited to a few weeks and emissions increased again towards mid of 2020.

In absolute numbers, concentration reductions were strongest for NO_2 in cities and for larger areas in the Po valley with more than 6 µg/m³ for a two weeks average in the second half of March. Northern Italy also showed the strongest relative decline with more than 50%. Rural areas in Germany, Poland and the Czech Republic showed the lowest reductions between 10% and 20%.

Ozone concentrations were often reduced, but not in cities and not in northern Europe between mid of March and beginning of April. This can be explained by reduced titration in cities (NO - O_3 reactions that destroy ozone) during the first phase of the lockdown, when NO emissions were lowest. The O_3 concentration changes were around +/- 5% which is much less than the NO_2 changes. The impacts of meteorological conditions can be much larger and the temporary O_3 increase in north eastern Europe in March would not have taken place under meteorological conditions as they were present in the years 2016 and 2018.

$PM_{2.5}$ concentrations were also decreased because of the lockdown emissions reductions, but the magnitude was much smaller than for NO_2, only between 2% and 10%. Particle bound nitrate contributes most to this effect. Again, concentration changes can be much larger due to meteorological conditions. The reductions in 2020 were relatively lower compared to the effects with 2016 and 2018 meteorological conditions.

Because the meteorological effects on concentrations of O_3 and $PM_{2.5}$ are larger than the lockdown emission reduction effects, it is difficult to judge or even quantify emission reduction effects by observations and comparison with previous years only. For NO_2, this is different, but in exceptional situations, like in February 2020, NO_2 can also be strongly influenced by meteorological conditions and lead to lower concentrations than in March during lockdown conditions.

Meteorological and chemistry transport models need to be applied to investigate the effects of emission reductions and separate them from meteorological effects. Although these models have deficiencies and systematic errors, e.g. underestimation of NO_2 and $PM_{2.5}$ concentrations, the impacts of emission changes caused by the lockdown can be quantified. The model accuracy is not sufficient to judge the correctness of the emission reduction estimates, however, the calculated NO_2 reductions agree well with estimations from ground based and satellite observations for Central Europe.

The emission reductions for several weeks during the first COVID-19 lockdown in Europe were the largest since decades. They can be seen as a huge test for emission reductions that could be achieved with significantly reduced

car traffic and air traffic. The reductions resulted in much lower NO_2 concentrations, particularly in cities, but the effects on secondary pollutants like ozone and $PM_{2.5}$ were limited and are hard to predict. The latter holds particularly for ozone that might even increase in some areas when traffic emissions are decreased. Systematic changes in prevailing weather situations that might appear due to climate change could mask effects of emission reductions on secondary pollutants. The relatively short duration of strong lockdown measures also results in limited effects on annual average NO_2 concentrations. Depending on location, only between 3% and 15% lower values could be reached.

Acknowledgements

The Community Air Quality Modeling System (CMAQ) is developed and maintained by the US EPA. Its use is gratefully acknowledged. J. Kuenen from TNO, Department of Climate, Air and Sustainability, is acknowledged for the provision of NMVOC splits for use with the CAMS-REGAP-EU emission inventory.
We thank to the weather mast group of the Meteorological Institute at the University of Hamburg, who delivered data from tower site Wettermast Hamburg.
We also thank the German Maritime and Hydrographic Agency for supporting us with AIS data taken in Bremerhaven, Hamburg and Kiel.

Author contribution

VM developed the idea, designed and supervised the study, evaluated part of the model results, prepared the manuscript and wrote most of the text. MQ co-designed the study, wrote most of the text about the meteorological situation and provided interpretations of the meteorology-chemistry interactions. JAA helped in designing the study, performed CMAQ model runs and provided code for the emission data preparation. RB developed the Lockdown Adjustment Factors, extrapolated emission data, and wrote the section about the emission data. LF performed CMAQ model runs, evaluated CMAQ model results and observation data and provided most of the plots. RP performed COSMO model runs, provided information for the meteorological data interpretation, wrote the text about the COSMO setup and part of the text about the meteorological situation, and analysed COSMO model results. JF developed emission extrapolation factors, and provided interpretation of the observational data. DS analysed AIS data and calculated ship emission LAFs. EML collected and analysed observational data and provided data interpretation. MR helped in designing the study, analysed and interpreted observational data for suburban stations. RW collected data on aviation emissions, provided LAFs for aviation and contributed to the discussion of the results

Code and data availability

The CMAQ model code is available through the CMAS Center https://www.cmascenter.org/cmaq/. The COSMO-CLM model is documented and available for members of the COSMO-CLM community at https://wiki.coast.hereon.de/clmcom . Lockdown adjustment factors (LAF) and projection factors (PF) as well as CMAQ model results are available upon request.

Competing interests

The authors declare no conflict of interest.

Appendix A

A1 Emission data

Table A1: Overview on available emission reduction information for countries in the investigated domain during the lockdown applied in this study

Country or Ocean Area	A_PublicPower	B_Industry	F_RoadTransport	G_Shipping	G_Shipping_Inland	H_Aviation
Albania					x	x
Austria	x	x	x		x	x
Baltic Sea				x		
Belarus			x		x	x
Belgium	x	x	x		x	x
Bosnia and Herzegowina	x		x		x	x
Bulgaria	x	x	x		x	x
Croatia	x	x	x		x	x
Cyprus	x				x	x
Czech Republic	x	x	x		x	x
Denmark	x	x	x		x	x
Estonia	x		x		x	x
Finland	x	x	x		x	x
France	x	x	x		x	x
Germany	x	x	x		x	x
Greece	x		x		x	x
Hungary	x	x	x		x	x
Iceland					x	x
Ireland	x		x		x	x
Italy	x	x	x		x	x
Latvia	x		x		x	x
Liechtenstein			x		x	
Lithuania	x		x		x	x
Luxembourg	x	x	x		x	x
Malta	x		x		x	x
Moldova			x		x	x

Montenegro	x				x	x
Netherlands	x	x	x		x	x
North Macedonia	x		x		x	x
North Sea				x		
Norway	x		x		x	x
Poland	x	x	x		x	x
Portugal	x	x	x		x	x
Romania	x	x	x		x	x
Russia			x		x	x
Serbia	x		x		x	x
Slovakia	x	x	x		x	x
Slovenia	x	x	x		x	x
Spain	x	x	x		x	x
Sweden	x		x		x	x
Switzerland	x		x		x	x
Turkey	x		x		x	x
United Kingdom	x	x	x		x	x
Ukraine			x		x	x

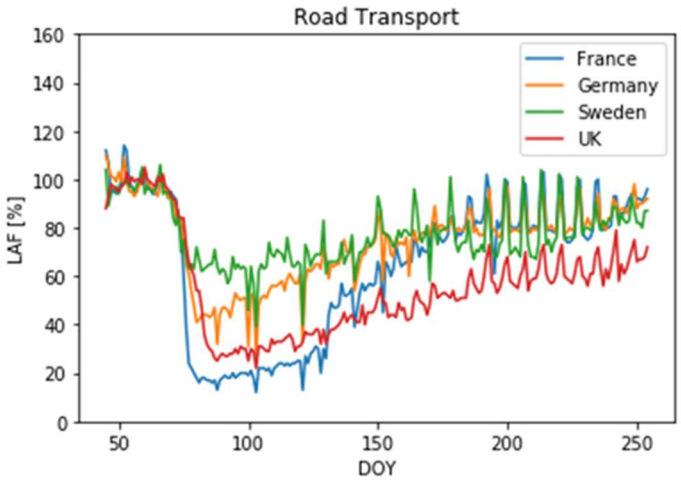

Figure A1: Daily values for Lockdown Adjustment Factors (in %) for the sector F_RoadTransport based on transit data from the Google Mobility Reports.

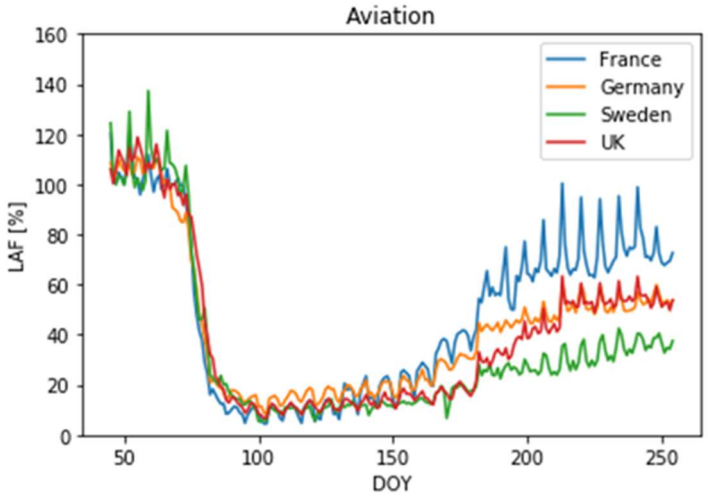

796

797 **Figure A2: Daily values for Lockdown Adjustment Factors (in %) for the sector H_Aviation based on Eurocontrol**
798 **data.**

799 **A2 Meteorological situation**

800 **Table A2: GWL classification for the period 1 Februray 2020 – 31 May 2020**

Date range	GWL
01.02. - 02.02.	Cyclonic Westerly
03.02. - 05.02.	Cyclonic North-Westerly
06.02. - 08.02.	High over Central Europe
09.02. - 12.02.	Cyclonic Westerly
13.02. - 16.02.	Anticyclonic South-Westerly
17.02. - 25.02.	Cyclonic Westerly
26.02. - 28.02.	Cyclonic North-Westerly
29.02. - 03.03.	Trough over Western Europe
04.03. - 06.03.	South-Shifted Westerly
07.03. - 09.03.	Maritime Westerly (Block E. Europe)
10.03. - 12.03.	Cyclonic Westerly
13.03. - 16.03.	Zonal Ridge across Central Europe
17.03. - 20.03.	Anticyclonic Westerly
21.03. - 26.03.	Scandinavian High Ridge C. Europe
27.03. - 29.03.	Anticyclonic North-Easterly
30.03. - 01.04.	Anticyclonic Northerly
02.04. - 04.04.	Anticyclonic North-Westerly
05.04. - 08.04.	Anticyclonic Southerly
09.04. - 11.04.	High over Central Europe
12.04.	undefined
13.04. - 15.04.	High over the British Isles
16.04. - 18.04.	Icelandic High Ridge C. Europe
19.04. - 23.04.	High Scandinavia-Iceland Ridge C. Europe
24.04. - 26.04.	Anticyclonic North-Westerly
27.04. - 29.04.	South-Shifted Westerly

30.04. - 02.05.	Cyclonic Westerly
03.05. - 05.05.	Anticyclonic Northerly
06.05. - 08.05.	High over Central Europe
09.05. - 12.05.	Icelandic High Trough C. Europe
13.05. - 15.05.	Anticyclonic North-Westerly
16.05. - 18.05.	Zonal Ridge across Central Europe
19.05. - 23.05.	High over Central Europe
24.05. - 27.05.	Anticyclonic Northerly
28.05. - 30.05.	Anticyclonic North-Easterly
31.05. - 02.06.	High Scandinavia-Iceland Ridge C. Europe

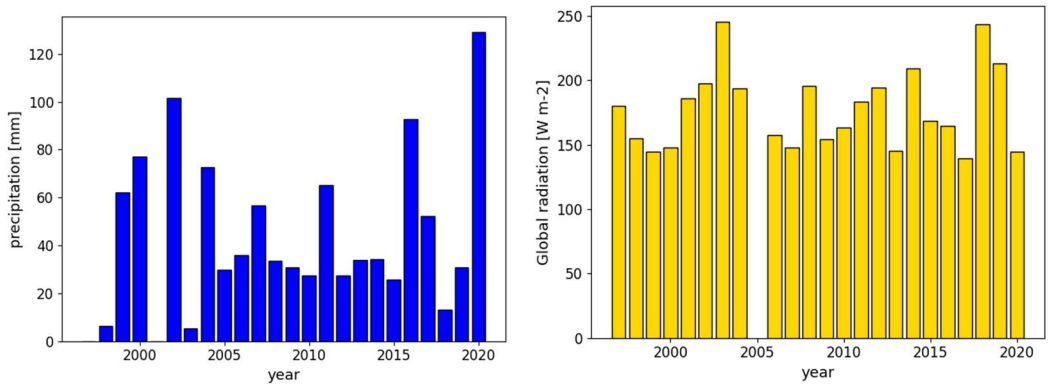

Figure A3: Time series of the monthly accumulated precipitation and mean solar irradiance between 10 and 14 UTC at the Wettermast Hamburg for February from 1997-2020.

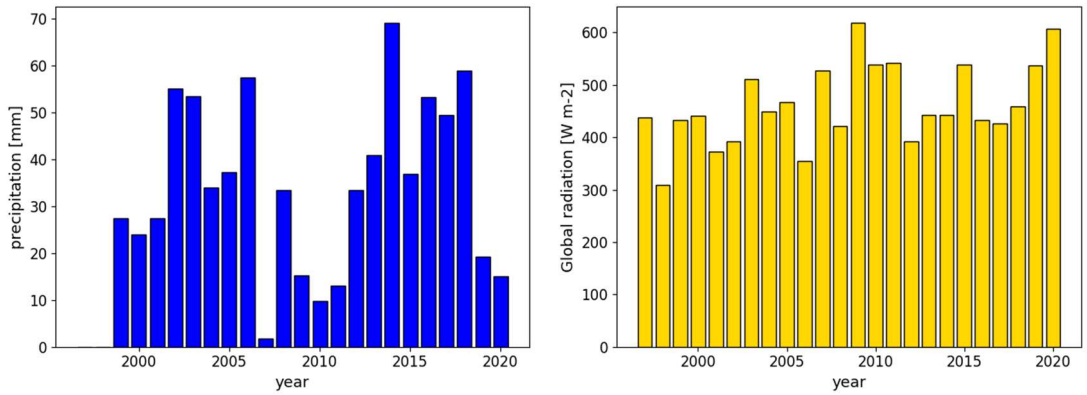

Figure A4: Time series of the monthly accumulated precipitation and mean solar irradiance between 10 and 14 UTC at the Wettermast Hamburg for April from 1997-2020.

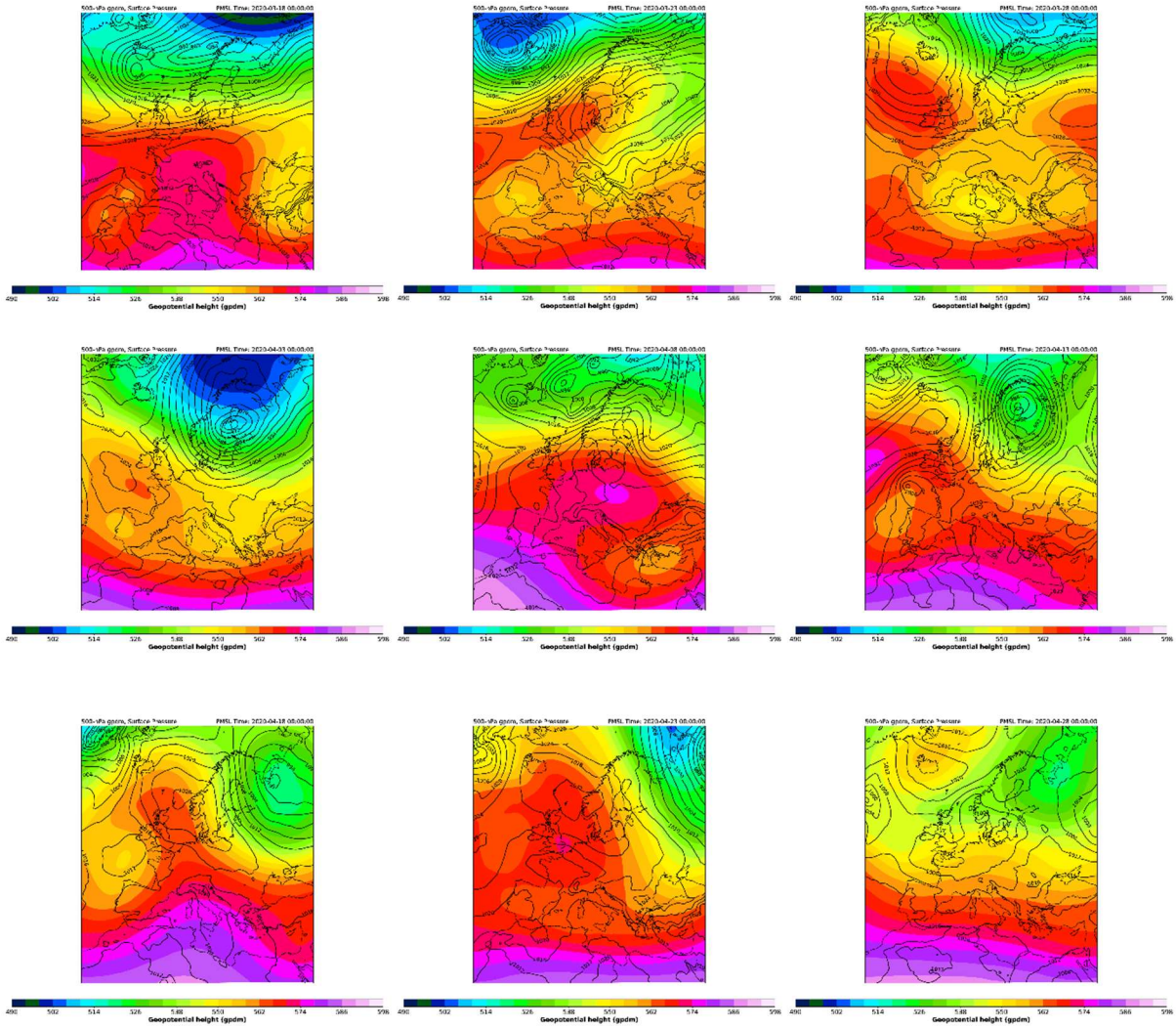

Figure A5: 500 hPa geopotential heights (in gpdm) and surface pressure (in hPa) for 4-days time segments in March and April 2020 according to the COSMO simulations. The geopotential heights are averaged over 4 days, displayed surface pressure distributions are representative snap shots within those time segments.

A3 COVID-19 lockdown effects

820

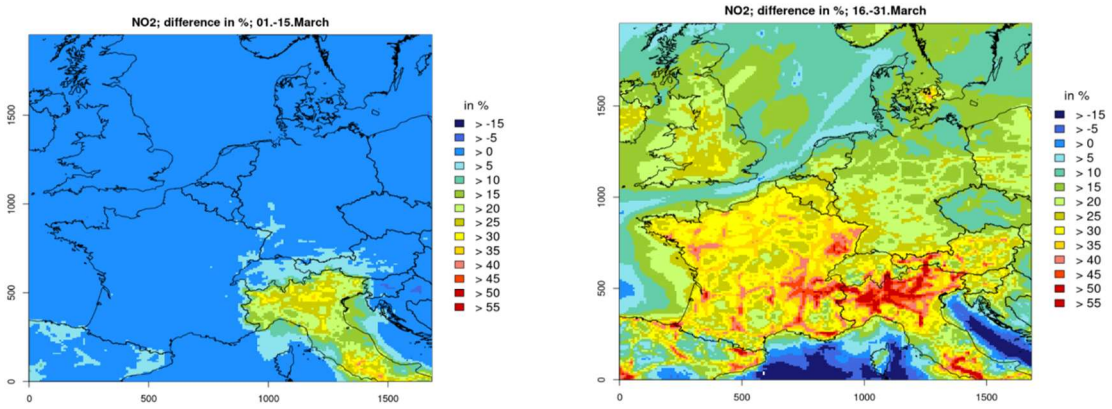

821

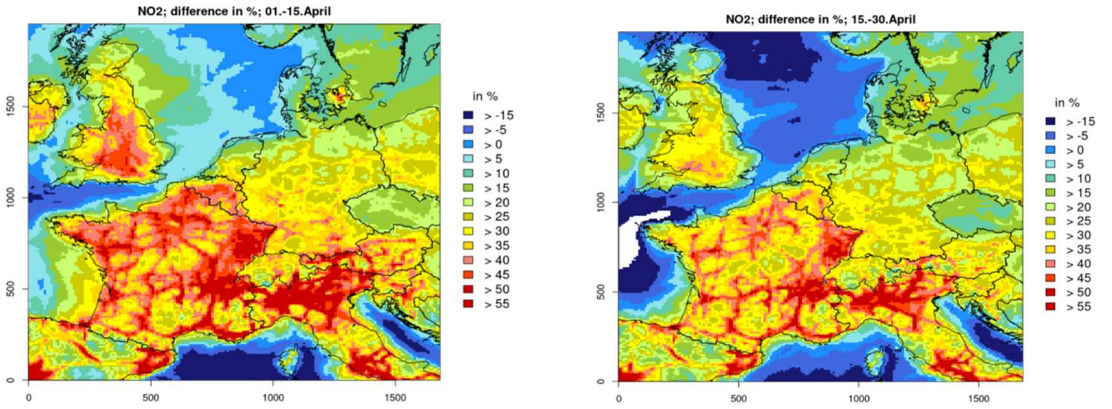

822

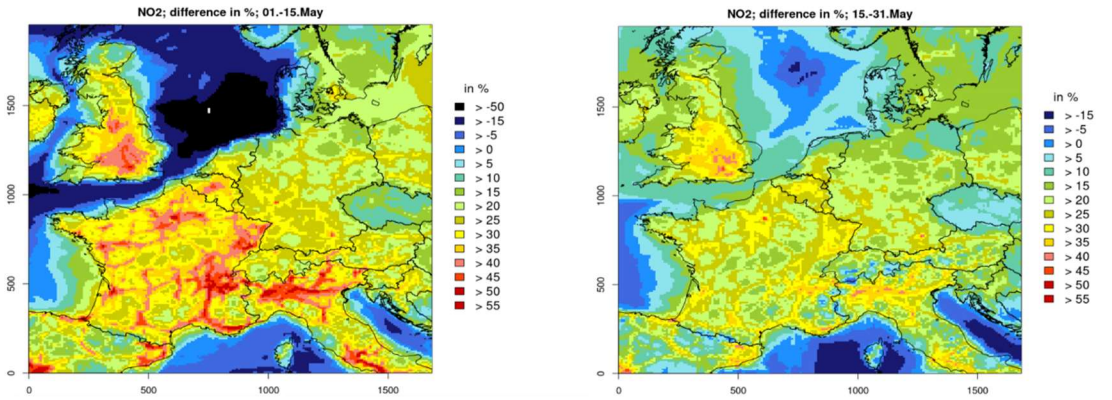

823 **Figure A6: CMAQ results for relative NO2 concentrations reductions due to lockdown measures (noCOV – COV run)**
824 **in Central Europe between 1 March and 31 May 2020 in half-monthly intervals; positive values denote reductions.**

825

826

827

828

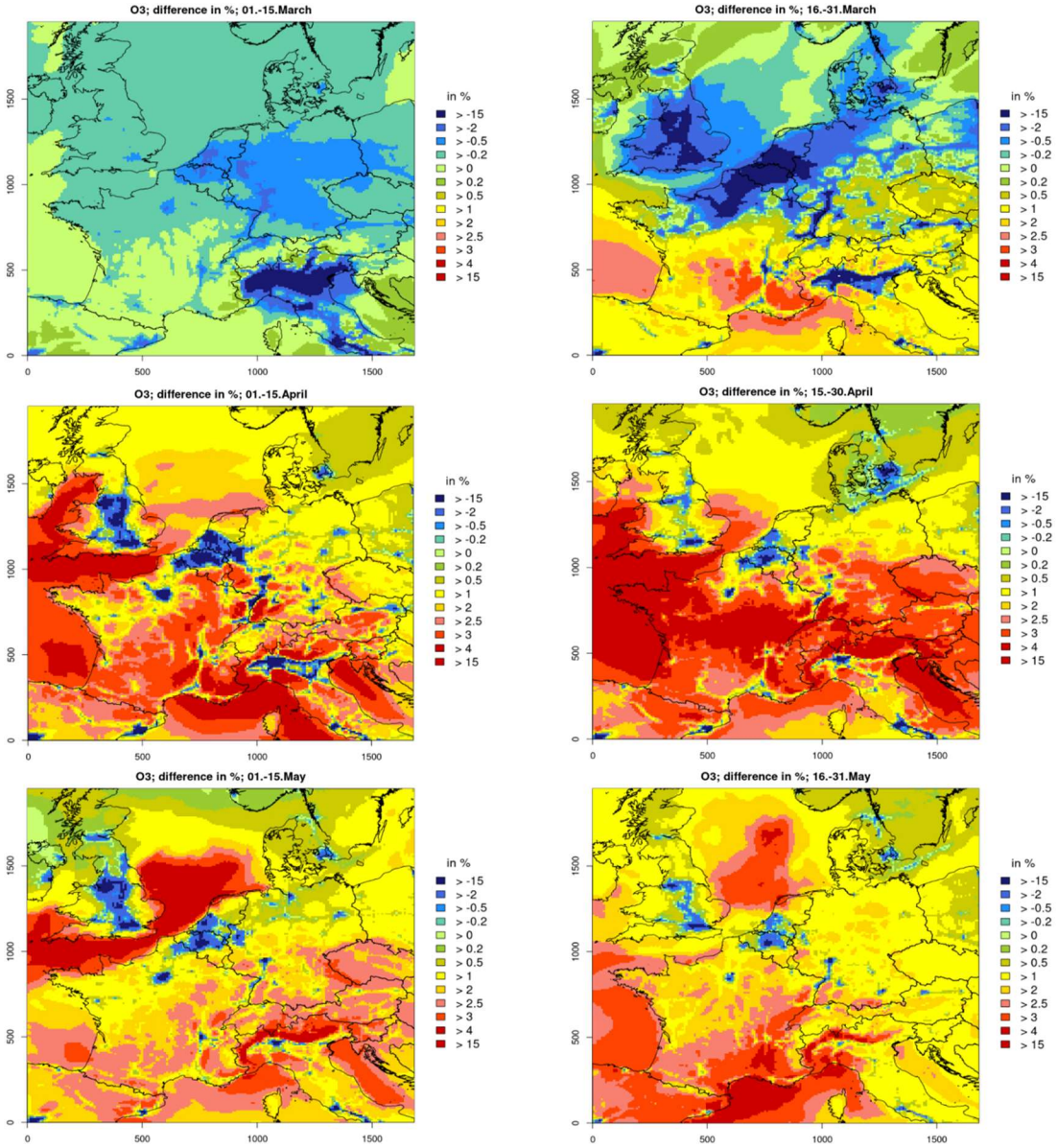

829 **Figure A7: CMAQ results for relative O_3 concentrations reductions due to lockdown measures (noCOV – COV run)**
830 **in Central Europe between 1 March and 31 May 2020 in half-monthly intervals; positive values denote reductions.**

831

832

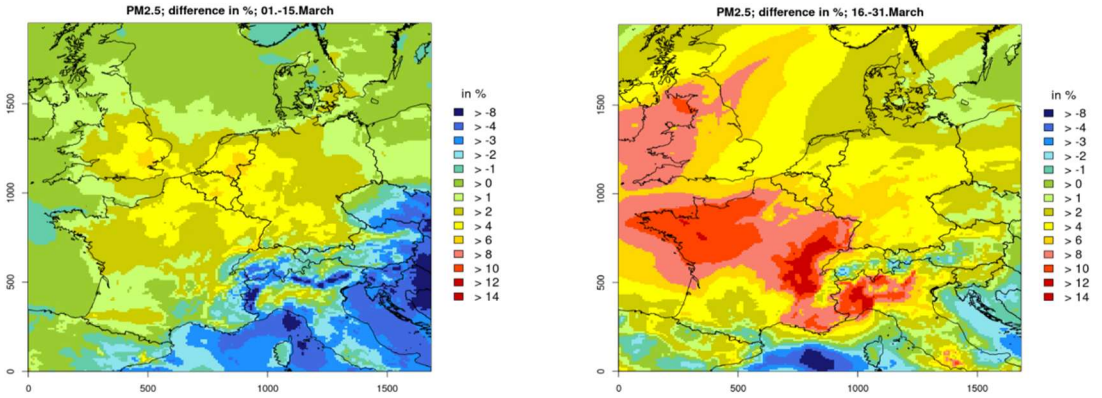

833

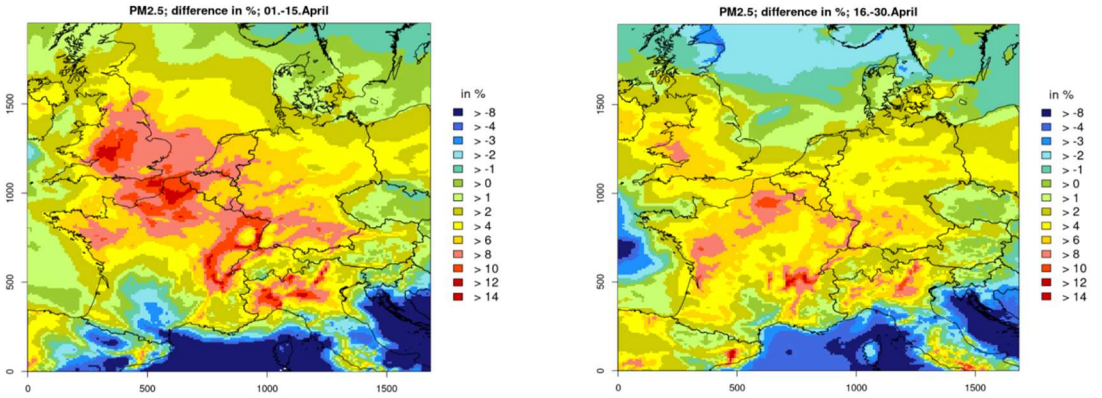

834

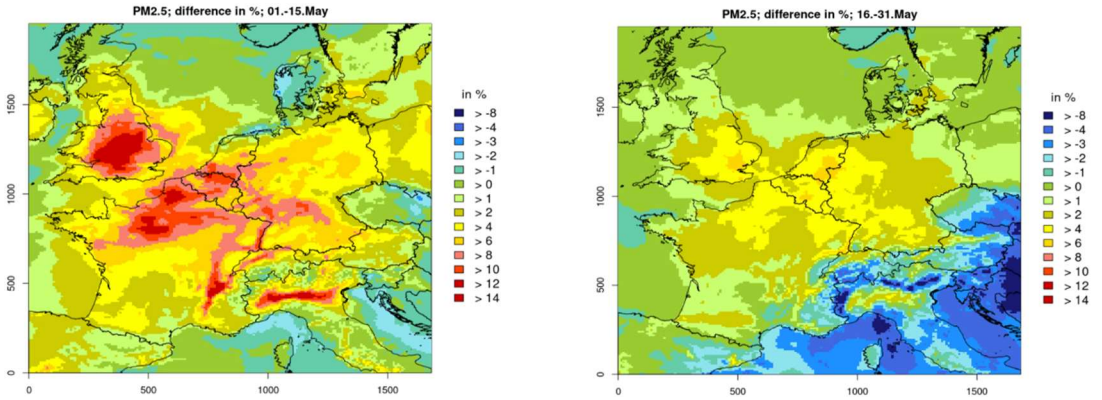

835 **Figure A8: CMAQ results for relative PM2.5 concentrations reductions due to lockdown measures (noCOV – COV**
836 **run) in Central Europe between 1 March and 31 May 2020 in half-monthly intervals; positive values denote reductions.**

837

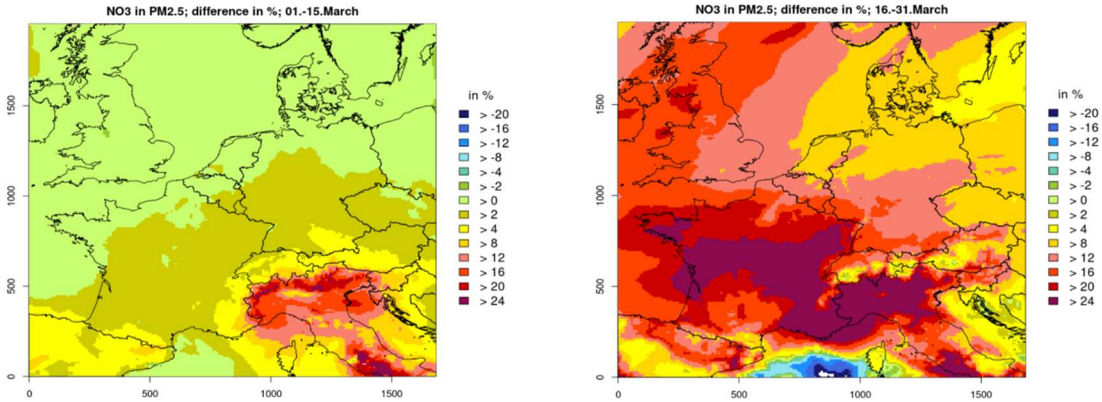

838

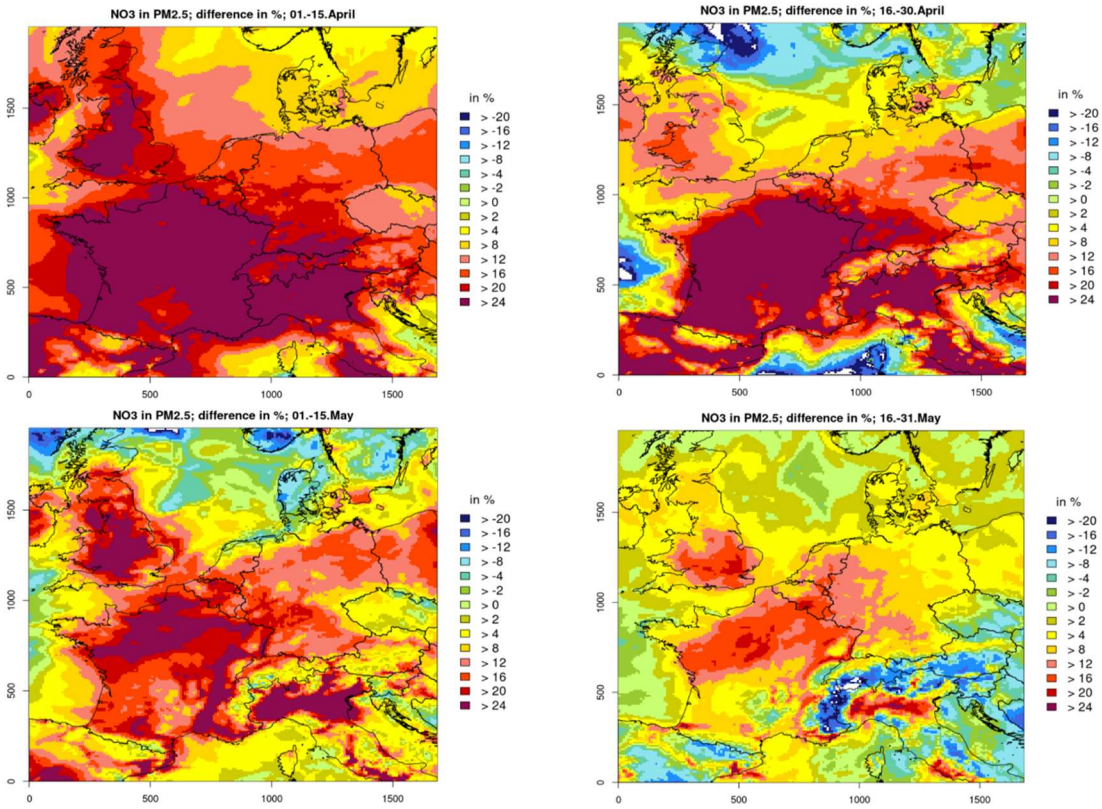

Figure A9: CMAQ results for relative particulate nitrate (NO_3^-) concentrations reductions due to lockdown measures (noCOV – COV run) in Central Europe between 1 March and 31 May 2020 in half-monthly intervals; positive values denote reductions.

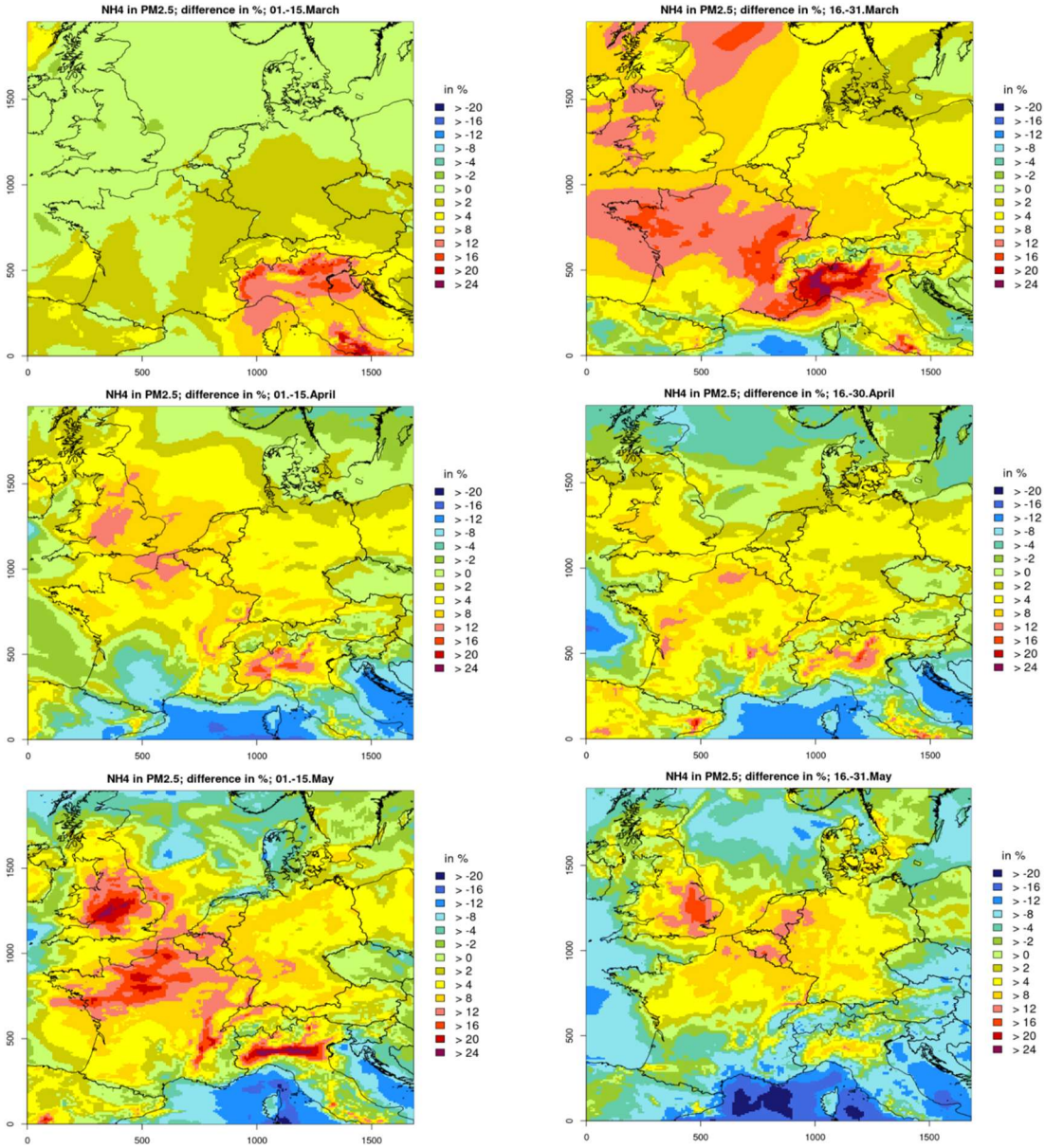

845
846
847

848 **Figure A10: CMAQ results for relative particulate ammonium (NH_4^+) concentrations reductions due to lockdown**
849 **measures (noCOV – COV run) in Central Europe between 1 March and 31 May 2020 in half-monthly intervals; positive**
850 **values denote reductions.**

851

852

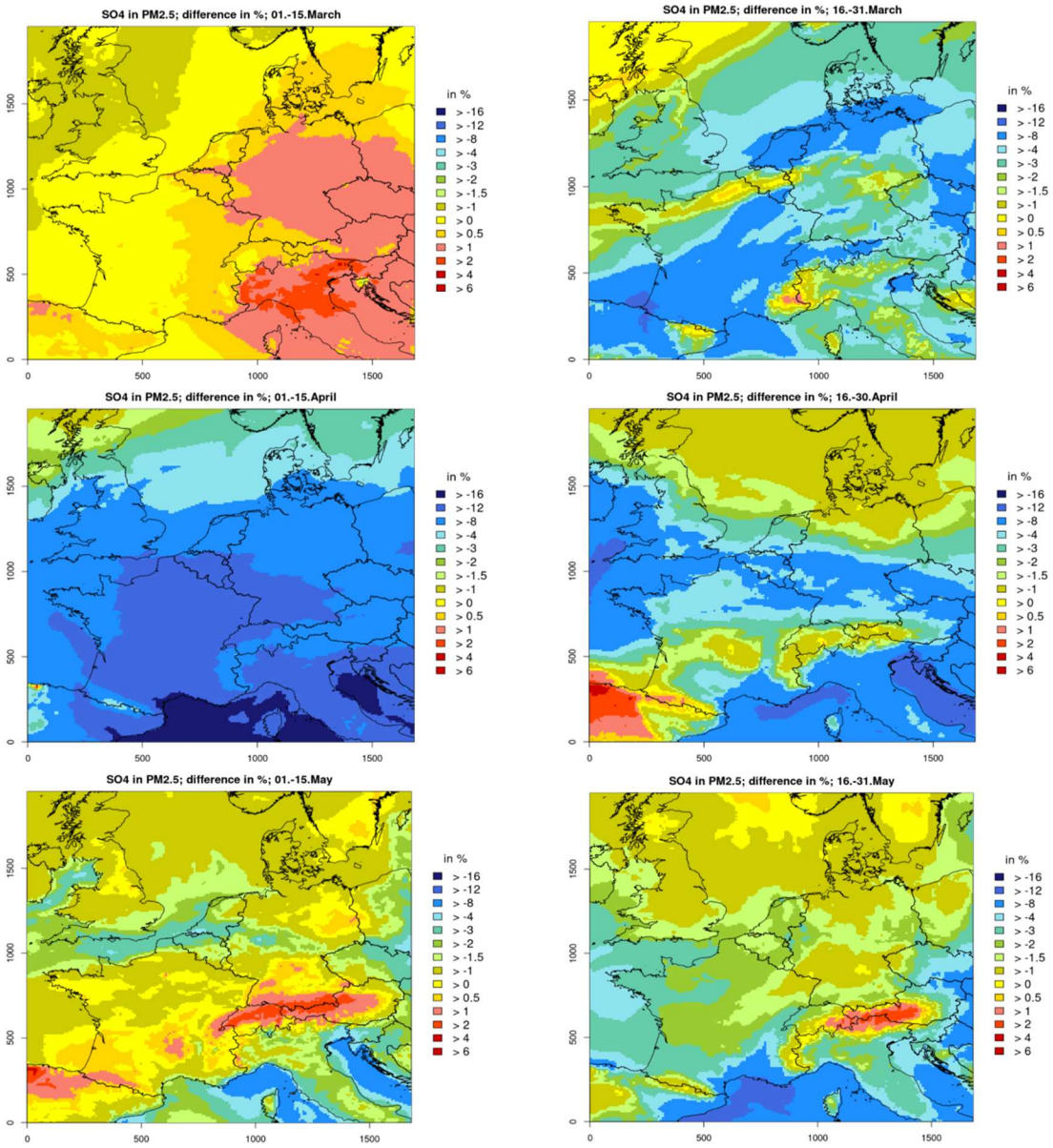

853

854

855 **Figure A11: CMAQ results for relative particulate sulfate (SO_4^{2-}) concentrations reductions due to lockdown measures**
856 **(noCOV – COV run) in Central Europe between 1 March and 31 May 2020 in half-monthly intervals; positive values**
857 **denote reductions.**

858

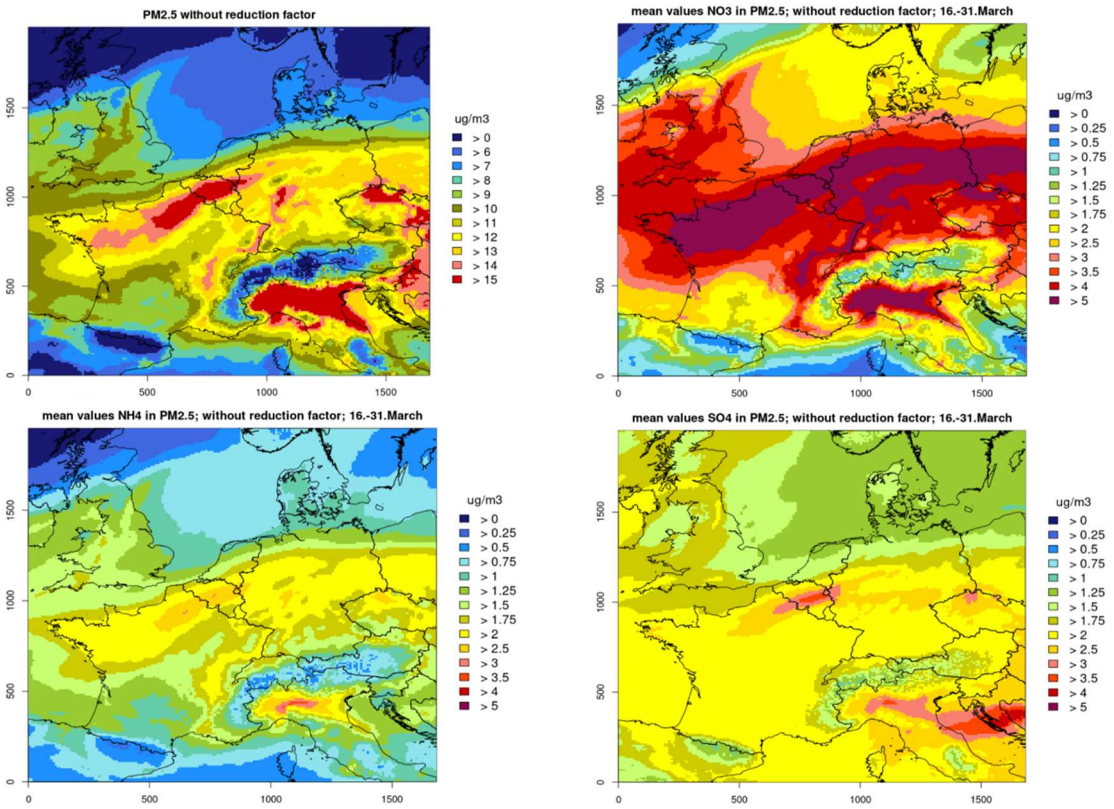

Figure A12: CMAQ results for concentrations of PM2.5 and its components nitrate, ammonium and sulphate in Central Europe between 16 March and 31 March 2020.

A4 Meteorological differences 2020 versus 2016 and 2018

In 2020 the geopotential height at 500 hPa over the British Isles and the North Sea was significantly higher compared to that in 2016, especially from 1 April onward. This resulted in a constellation which favours blocking in 2020. Near surface high pressure systems were amplified and more persistent and weak wind conditions and a more continental flow dominate. In 2016 stronger winds of Atlantic origin occasionally were observed. In 2020 precipitation was considerably lower compared to 2016. In most parts of the study region solar radiation was clearly higher in 2020, especially over Central Europe up to the British Isles.

Much of what was has been said concerning the blocking condition in 2020 holds as well when compared to 2018. The year 2020 also was much drier and incoming solar radiation was more intense. In 2018 winds had a more easterly to south-easterly component. The spatial and temporal distribution and the absolute values of the meteorological parameters were slightly different in 2018 compared to 2016 (see Fig. A13- A15), so this year became an additional choice for the evaluation of meteorological influences.

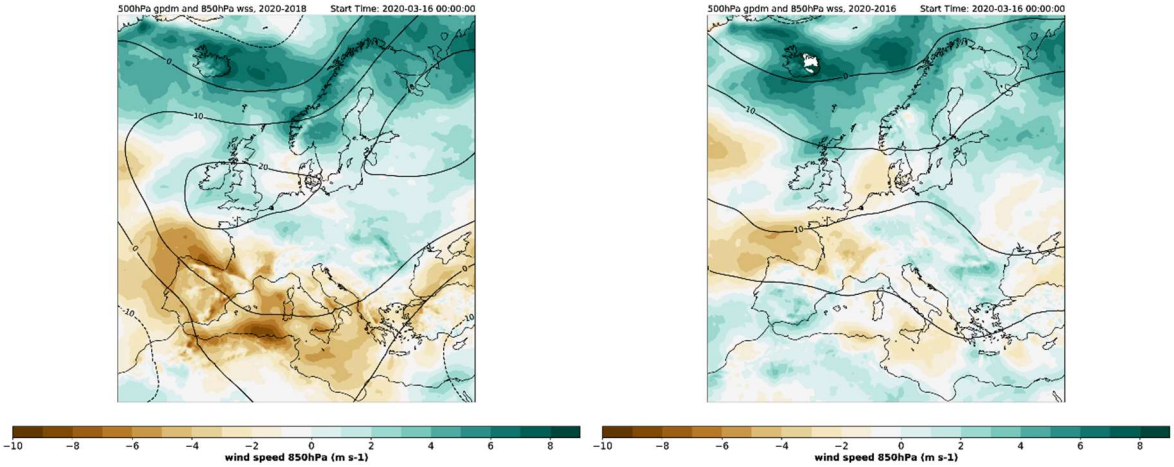

878

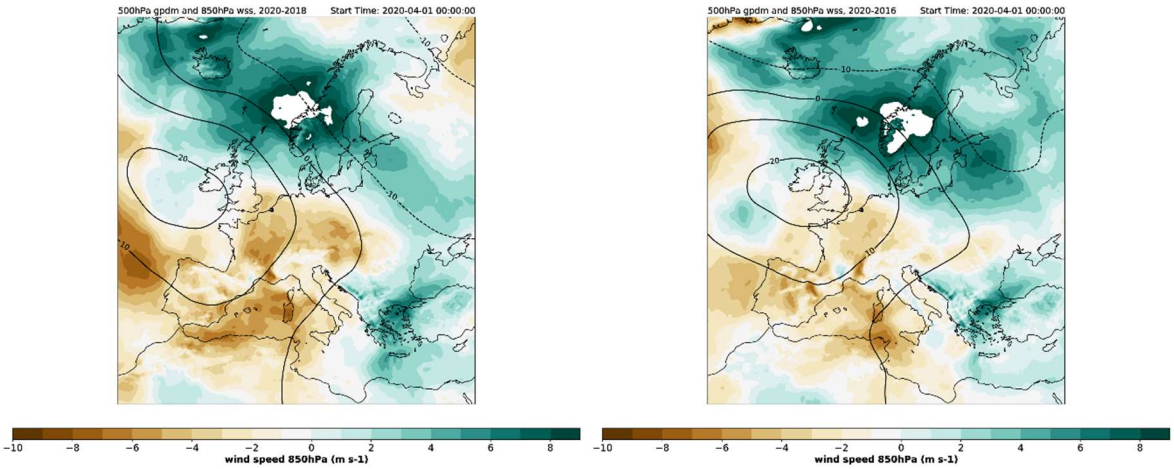

879

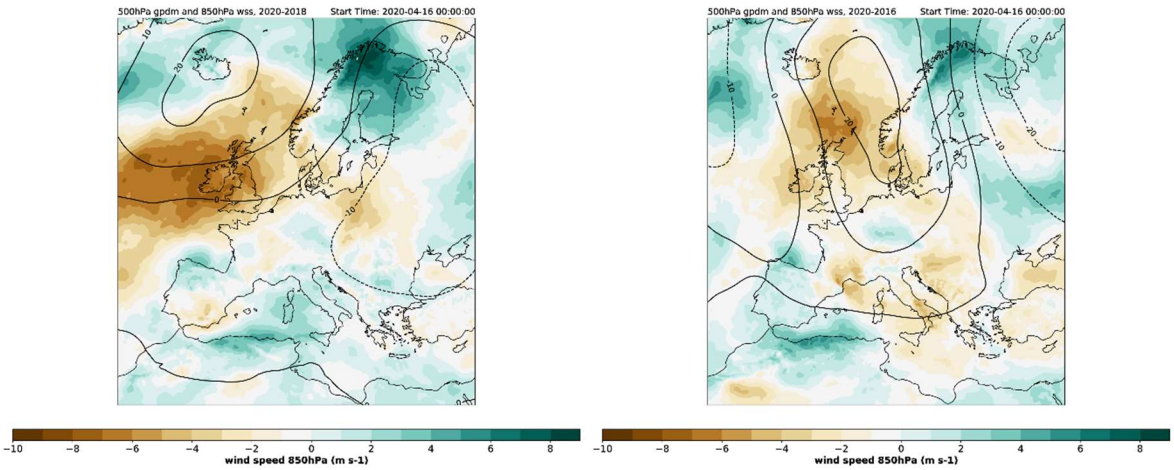

880

881 **Figure A13: Geopotential height at 500 hPa (in gpdm, isolines) and windspeed at 850 hPa (in m/s, color code):**
882 **Differences between 2020 and 2018 (left column) and 2020 and 2016 (right column) for the half month-periods 16 macrh**
883 **– 31 March (top), 1 April – 15 April (middle) and 16 April – 30 April (bottom).**

884

885

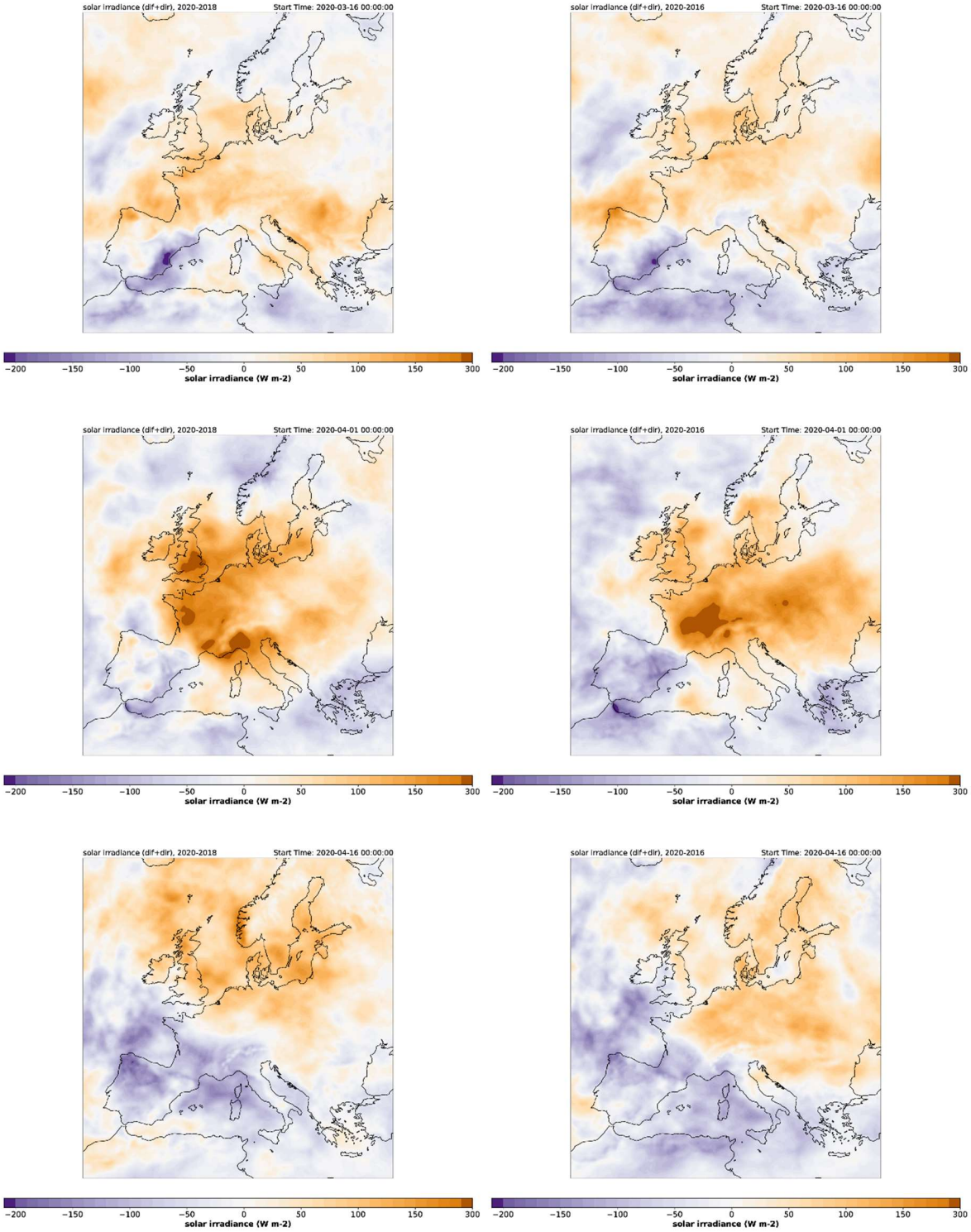

Figure A14: Solar irradiance (in W/m², color code): Differences between 2020 and 2018 (left column) and 2020 and 2016 (right column) for the half month-periods 16 March – 31 March (top), 1 April – 15 April (middle) and 16 April – 30 April (bottom).

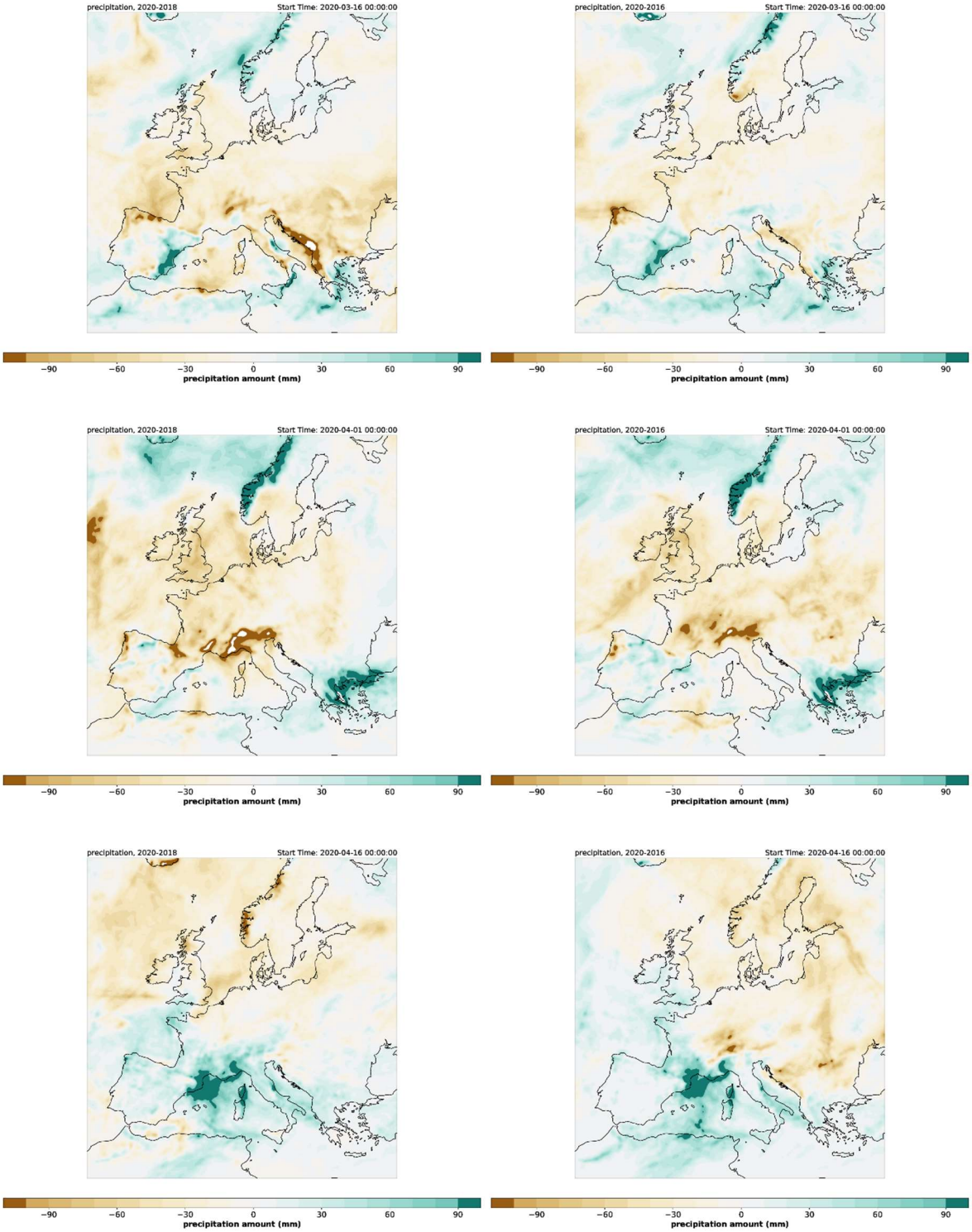

Figure A15: Accumulated precipitation (in mm, color code): Differences between 2020 and 2018 (left column) and 2020 and 2016 (right column) for the half month-periods 16 March – 31 March (top), 1 April – 15 April (middle) and 16 April – 30 April (bottom).

References

Amouei Torkmahalleh, M., Akhmetvaliyeva, Z., Omran, A. D., Faezeh Darvish Omran, F., Kazemitabar, M., Naseri, M., Naseri, M., Sharifi, H., Malekipirbazari, M., Kwasi Adotey, E., Gorjinezhad, S., Eghtesadi, N., Sabanov, S., Alastuey, A., de Fátima Andrade, M., Buonanno, G., Carbone, S., Cárdenas-Fuentes, D. E., Cassee, F. R., Dai, Q., Henríquez, A., Hopke, P. K., Keronen, P., Khwaja, H. A., Kim, J., Kulmala, M., Kumar, P., Kushta, J., Kuula, J., Massagué, J., Mitchell, T., Mooibroek, D., Morawska, L., Niemi, J. V., Ngagine, S. H., Norman, M., Oyama, B., Oyola, P., Öztürk, F., Petäjä, T., Querol, X., Rashidi, Y., Reyes, F., Ross-Jones, M., Salthammer, T., Savvides, C., Stabile, L., Sjöberg, K., Söderlund, K., Sunder Raman, R., Timonen, H., Umezawa, M., Viana, M., and Xie, S.: Global Air Quality and COVID-19 Pandemic: Do We Breathe Cleaner Air?, Aerosol and Air Quality Research, 21, 200567, 10.4209/aaqr.200567, 2021.

Baldauf, M., Seifert, A., Forstner, J., Majewski, D., Raschendorfer, M., and Reinhardt, T.: Operational Convective-Scale Numerical Weather Prediction with the COSMO Model: Description and Sensitivities, Monthly Weather Review, 139, 3887-3905, 10.1175/mwr-d-10-05013.1, 2011.

Baret, F., Weiss, M., Lacaze, R., Camacho, F., Makhmara, H., Pacholcyzk, P., and Smets, B.: GEOV1: LAI and FAPAR essential climate variables and FCOVER global time series capitalizing over existing products. Part1: Principles of development and production, Remote Sensing of Environment, 137, 299-309, 10.1016/j.rse.2012.12.027, 2013.

Bauwens, M., Compernolle, S., Stavrakou, T., Muller, J. F., van Gent, J., Eskes, H., Levelt, P. F., van der, A. R., Veefkind, J. P., Vlietinck, J., Yu, H., and Zehner, C.: Impact of coronavirus outbreak on NO2 pollution assessed using TROPOMI and OMI observations, Geophys Res Lett, e2020GL087978, 10.1029/2020GL087978, 2020.

Bessagnet, B., Pirovano, G., Mircea, M., Cuvelier, C., Aulinger, A., Calori, G., Ciarelli, G., Manders, A., Stern, R., Tsyro, S., Vivanco, M. G., Thunis, P., Pay, M. T., Colette, A., Couvidat, F., Meleux, F., Rouil, L., Ung, A., Aksoyoglu, S., Baldasano, J. M., Bieser, J., Briganti, G., Cappelletti, A., D'Isidoro, M., Finardi, S., Kranenburg, R., Silibello, C., Carnevale, C., Aas, W., Dupont, J. C., Fagerli, H., Gonzalez, L., Menut, L., Prevot, A. S. H., Roberts, P., and White, L.: Presentation of the EURODELTA III intercomparison exercise - evaluation of the chemistry transport models' performance on criteria pollutants and joint analysis with meteorology, Atmospheric Chemistry and Physics, 16, 12667-12701, 10.5194/acp-16-12667-2016, 2016.

Bieser, J., Aulinger, A., Matthias, V., Quante, M., and Builtjes, P.: SMOKE for Europe - adaptation, modification and evaluation of a comprehensive emission model for Europe, Geoscientific Model Development, 3, 949-1007, 2010.

Bieser, J., Aulinger, A., Matthias, V., Quante, M., and Denier van der Gon, H. A. C.: Vertical emission profiles for Europe based on plume rise calculations, Environmental Pollution, 159, 2935-2946, 2011.

Bissolli, P., and Dittmann, E.: The objective weather type classification of the German Weather Service and its possibilities of application to environmental and meteorological investigations, Meteorologische Zeitschrift, 10, 253-260, 10.1127/0941-2948/2001/0010-0253, 2001.

Brümmer, B., and Schultze, M.: Analysis of a 7-year low-level temperature inversion data set measured at the 280 m high Hamburg weather mast, Meteorologische Zeitschrift, 24, 481-494, 10.1127/metz/2015/0669, 2015.

939 Byun, D., and Schere, K. L.: Review of the Governing Equations, Computational Algorithms, and Other
940 Components of the Models-3 Community Multiscale Air Quality (CMAQ) Modeling System, Applied Mechanics
941 Reviews, 59, 51-77, 2006.
942 Byun, D. W., and Ching, J. K. S.: Science Algorithms of the EPA Models-3 Community Multiscale Air Quality
943 Modeling System, 1999.
944 Collivignarelli, M. C., Abba, A., Caccamo, F. M., Bertanza, G., Pedrazzani, R., Baldi, M., Ricciardi, P., and
945 Miino, M. C.: Can particulate matter be identified as the primary cause of the rapid spread of CoViD-19 in some
946 areas of Northern Italy?, Environmental Science and Pollution Research, 10.1007/s11356-021-12735-x, 2020.
947 Denier van der Gon, H. A. C., Hendriks, C., Kuenen, J., Segers, A., and Visschedijk, A.: Description of current
948 temporal emission patterns and sensitivity of predicted AQ for temporal emission patternsEU FP7 MACC
949 deliverable report D_D-EMIS_1.3, 2011.
950 Deroubaix, A., Brasseur, G., Gaubert, B., Labuhn, I., Menut, L., Siour, G., and Tuccella, P.: Response of surface
951 ozone concentration to emission reduction and meteorology during the COVID-19 lockdown in Europe,
952 Meteorological Applications, 28, e1990, https://doi.org/10.1002/met.1990, 2021.
953 Doms, G., and Schättler, U.: A Description of the Nonhydrostatic Regional Model LM. Part I: Dynamics and
954 Numerics, 2002.
955 Doms, G., Foerstner, J., Heise, E., Herzog, H. J., Mrionow, D., Raschendorfer, M., Reinhart, T., Ritter, B.,
956 Schrodin, R., Schulz, J. P., and Vogel, G.: A Description of the Nonhydrostatic Regional COSMO Model. Part II:
957 Physical Parameterization, 2011.
958 Doumbia, T., Granier, C., Elguindi, N., Bouarar, I., Darras, S., Brasseur, G., Gaubert, B., Liu, Y., Shi, X.,
959 Stavrakou, T., Tilmes, S., Lacey, F., Deroubaix, A., and Wang, T.: Changes in global air pollutant emissions
960 during the COVID-19 pandemic: a dataset for atmospheric chemistry modeling, Earth Syst. Sci. Data Discuss.,
961 2021, 1-26, 10.5194/essd-2020-348, 2021.
962 Forster, P. M., Forster, H. I., Evans, M. J., Gidden, M. J., Jones, C. D., Keller, C. A., Lamboll, R. D., Quéré, C.
963 L., Rogelj, J., Rosen, D., Schleussner, C.-F., Richardson, T. B., Smith, C. J., and Turnock, S. T.: Current and
964 future global climate impacts resulting from COVID-19, Nature Climate Change, 10, 913-919, 10.1038/s41558-
965 020-0883-0, 2020.
966 Gaubert, B., Bouarar, I., Doumbia, T., Liu, Y., Stavrakou, T., Deroubaix, A., Darras, S., Elguindi, N., Granier, C.,
967 Lacey, F., Müller, J.-F., Shi, X., Tilmes, S., Wang, T., and Brasseur, G. P.: Global Changes in Secondary
968 Atmospheric Pollutants During the 2020 COVID-19 Pandemic, Journal of Geophysical Research: Atmospheres,
969 126, e2020JD034213, https://doi.org/10.1029/2020JD034213, 2021.
970 Gelaro, R., McCarty, W., Suarez, M. J., Todling, R., Molod, A., Takacs, L., Randles, C. A., Darmenov, A.,
971 Bosilovich, M. G., Reichle, R., Wargan, K., Coy, L., Cullather, R., Draper, C., Akella, S., Buchard, V., Conaty,
972 A., da Silva, A. M., Gu, W., Kim, G. K., Koster, R., Lucchesi, R., Merkova, D., Nielsen, J. E., Partyka, G., Pawson,
973 S., Putman, W., Rienecker, M., Schubert, S. D., Sienkiewicz, M., and Zhao, B.: The Modern-Era Retrospective
974 Analysis for Research and Applications, Version 2 (MERRA-2), Journal of Climate, 30, 5419-5454, 10.1175/jcli-
975 d-16-0758.1, 2017.
976 Gkatzelis, G. I., Gilman, J. B., Brown, S. S., Eskes, H., Gomes, A. R., Lange, A. C., McDonald, B. C., Peischl, J.,
977 Petzold, A., Thompson, C. R., and Kiendler-Scharr, A.: The global impacts of COVID-19 lockdowns on urban

air pollution: A critical review and recommendations, Elementa: Science of the Anthropocene, 9, 10.1525/elementa.2021.00176, 2021.

Goldberg, D. L., Anenberg, S. C., Griffin, D., McLinden, C. A., Lu, Z., and Streets, D. G.: Disentangling the Impact of the COVID-19 Lockdowns on Urban NO2 From Natural Variability, Geophysical Research Letters, 47, e2020GL089269, https://doi.org/10.1029/2020GL089269, 2020.

Guenther, A., Jiang, X., Shah, T., Huang, L., S. Kemball-Cook, and Yarwood, G.: Model of Emissions of Gases and Aerosol from Nature Version 3 (MEGAN3) for Estimating Biogenic Emissions, Air Pollution Modeling and Its Application XXVI, edited by: Mensink, C., Gong, W., and Hakami, A., Springer International Publishing, Cham, 187-192 pp., 2020.

Guenther, A. B., Jiang, X., Heald, C. L., Sakulyanontvittaya, T., Duhl, T., Emmons, L. K., and Wang, X.: The Model of Emissions of Gases and Aerosols from Nature version 2.1 (MEGAN2.1): an extended and updated framework for modeling biogenic emissions, Geoscientific Model Development, 5, 1471-1492, 2012.

Guevara, M., Jorba, O., Soret, A., Petetin, H., Bowdalo, D., Serradell, K., Tena, C., Denier van der Gon, H., Kuenen, J., Peuch, V. H., and Pérez García-Pando, C.: Time-resolved emission reductions for atmospheric chemistry modelling in Europe during the COVID-19 lockdowns, Atmos. Chem. Phys., 21, 773-797, 10.5194/acp-21-773-2021, 2021.

Hess, P., and Brezowsky, H.: Katalog der Großwetterlagen Europas, Offenbach a.M., , 14 & 54, 1977.

Huang, X., Ding, A., Gao, J., Zheng, B., Zhou, D., Qi, X., Tang, R., Wang, J., Ren, C., Nie, W., Chi, X., Xu, Z., Chen, L., Li, Y., Che, F., Pang, N., Wang, H., Tong, D., Qin, W., Cheng, W., Liu, W., Fu, Q., Liu, B., Chai, F., Davis, S. J., Zhang, Q., and He, K.: Enhanced secondary pollution offset reduction of primary emissions during COVID-19 lockdown in China, National Science Review, 10.1093/nsr/nwaa137, 2020.

Inness, A., Ades, M., Agustí-Panareda, A., Barré, J., Benedictow, A., Blechschmidt, A., Dominguez, J., Engelen, R., Eskes, H., Flemming, J., Huijnen, V., Jones, L., Kipling, Z., Massart, S., Parrington, M., Peuch, V.-H., M, R., Remy, S., Schulz, M., and Suttie, M.: CAMS global reanalysis (EAC4). , in, edited by: (ADS), C. A. M. S. C. A. D. S., 2019a.

Inness, A., Ades, M., Agusti-Panareda, A., Barre, J., Benedictow, A., Blechschmidt, A. M., Dominguez, J. J., Engelen, R., Eskes, H., Flemming, J., Huijnen, V., Jones, L., Kipling, Z., Massart, S., Parrington, M., Pench, V. H., Razinger, M., Remy, S., Schulz, M., and Suttie, M.: The CAMS reanalysis of atmospheric composition, Atmospheric Chemistry and Physics, 19, 3515-3556, 10.5194/acp-19-3515-2019, 2019b.

James, P. M.: An objective classification method for Hess and Brezowsky Grosswetterlagen over Europe, Theoretical and Applied Climatology, 88, 17-42, 10.1007/s00704-006-0239-3, 2007.

Kelly, J. T., Bhave, P. V., Nolte, C. G., Shankar, U., and Foley, K. M.: Simulating emission and chemical evolution of coarse sea-salt particles in the Community Multiscale Air Quality (CMAQ) model, Geoscientific Model Development, 3, 257-273, 2010.

Kroll, J. H., Heald, C. L., Cappa, C. D., Farmer, D. K., Fry, J. L., Murphy, J. G., and Steiner, A. L.: The complex chemical effects of COVID-19 shutdowns on air quality, Nat Chem, 12, 777-779, 10.1038/s41557-020-0535-z, 2020.

Le Quéré, C., Jackson, R. B., Jones, M. W., Smith, A. J. P., Abernethy, S., Andrew, R. M., De-Gol, A. J., Willis, D. R., Shan, Y., Canadell, J. G., Friedlingstein, P., Creutzig, F., and Peters, G. P.: Temporary reduction in daily

global CO2 emissions during the COVID-19 forced confinement, Nature Climate Change, 10, 647-653, 10.1038/s41558-020-0797-x, 2020.
Lonati, G., and Riva, F.: Regional Scale Impact of the COVID-19 Lockdown on Air Quality: Gaseous Pollutants in the Po Valley, Northern Italy, Atmosphere, 12, 264, 2021.
Matthias, V., Arndt, J. A., Aulinger, A., Bieser, J., van der Gon, H. D., Kranenburg, R., Kuenen, J., Neumann, D., Pouliot, G., and Quante, M.: Modeling emissions for three-dimensional atmospheric chemistry transport models, Journal of the Air & Waste Management Association, 68, 763-800, 10.1080/10962247.2018.1424057, 2018.
Menut, L., Bessagnet, B., Siour, G., Mailler, S., Pennel, R., and Cholakian, A.: Impact of lockdown measures to combat Covid-19 on air quality over western Europe, Sci Total Environ, 741, 140426, 10.1016/j.scitotenv.2020.140426, 2020.
Mertens, M., Jöckel, P., Matthes, S., Nützel, M., Grewe, V., and Sausen, R.: COVID-19 induced lower-tropospheric ozonechanges, Environ. Res. Lett., in press, 10.1088/1748-9326/abf191, 2021.
Petetin, H., Bowdalo, D., Soret, A., Guevara, M., Jorba, O., Serradell, K., and Garcia-Pando, C. P.: Meteorology-normalized impact of the COVID-19 lockdown upon NO2 pollution in Spain, Atmospheric Chemistry and Physics, 20, 11119-11141, 10.5194/acp-20-11119-2020, 2020.
Petrik, R., Geyer, B., and Rockel, B.: On the diurnal cycle and variability of winds in the lower planetary boundary layer: evaluation of regional reanalyses and hindcasts, Tellus Series a-Dynamic Meteorology and Oceanography, 73, 1-28, 10.1080/16000870.2020.1804294, 2021.
Rockel, B., Will, A., and Hense, A.: The Regional Climate Model COSMO-CLM(CCLM), Meteorologische Zeitschrift, 17, 347-348, 2008.
Schwarzkopf, D. A., Petrik, R., Matthias, V., and Quante, M.: A Ship Emission Modeling System with Scenario Capabilities, Atmospheric Environment X, under review, 2021.
Sharma, S., Zhang, M., Anshika, Gao, J., Zhang, H., and Kota, S. H.: Effect of restricted emissions during COVID-19 on air quality in India, Sci Total Environ, 728, 138878, 10.1016/j.scitotenv.2020.138878, 2020.
Solazzo, E., Bianconi, R., Pirovano, G., Matthias, V., Vautard, R., Moran, M. D., Appel, K. W., Bessagnet, B., Brandt, J., Christensen, J. H., Chemel, C., Coll, I., Ferreira, J., Forkel, R., Francis, X. V., Grell, G., Grossi, P., Hansen, A. B., Miranda, A. I., Nopmongcol, U., Prank, M., Sartelet, K. N., Schaap, M., Silver, J. D., Sokhi, R. S., Vira, J., Werhahn, J., Wolke, R., Yarwood, G., Zhang, J., Rao, S. T., and Galmarini, S.: Operational model evaluation for particulate matter in Europe and North America in the context of AQMEII, Atmospheric Environment, 53, 75-92, 2012.
van Heerwaarden, C. C., Mol, W. B., Veerman, M. A., Benedict, I., Heusinkveld, B. G., Knap, W. H., Kazadzis, S., Kouremeti, N., and Fiedler, S.: Record high solar irradiance in Western Europe during first COVID-19 lockdown largely due to unusual weather, Communications Earth & Environment, 2, 37, 10.1038/s43247-021-00110-0, 2021.
Velders, G. J. M., Willers, S. M., Wesseling, J., den Elshout, S. v., van der Swaluw, E., Mooibroek, D., and van Ratingen, S.: Improvements in air quality in the Netherlands during the corona lockdown based on observations and model simulations, Atmospheric Environment, 247, 10.1016/j.atmosenv.2020.118158, 2021.